Chemical Engineering Research and Design 223 (2025) 311–330

Contents lists available at ScienceDirect

Chemical Engineering Research and Design

journal homepage: www.elsevier.com/locate/cherd

Feature-based scenario clustering and selective degrees of freedom reduction for two-stage stochastic optimization of Power-to-Methanol ☆

Simone Mucci [a,b], Dominik Bongartz [b,c,*]

[a] Process Systems Engineering (AVT.SVT), RWTH Aachen University, 52074 Aachen, Germany
[b] Department of Chemical Engineering, KU Leuven, 3001 Leuven, Belgium
[c] EnergyVille, 3600 Genk, Belgium

ARTICLE INFO

Keywords:
Two-stage stochastic programming
Combined design and scheduling
Scenario clustering
Degrees of freedom reduction
k-medoids
Power-to-Methanol

ABSTRACT

Power-to-X processes can be operated flexibly to exploit electricity price fluctuations or renewable power availability, reducing production costs. Ideally, the process design should be optimized simultaneously with the scheduling or operation. To address the uncertainty in electricity prices or availability, several scheduling scenarios can be simultaneously considered in two-stage stochastic optimization problems. However, these problems, especially when nonlinear, become challenging to solve when the scenario number and scheduling horizon increase.

To tackle this challenge, we combine feature-based scenario clustering with reducing the degrees of freedom (DoF) related to the scheduling variables. The latter maintains time step chronology memory, thus ensuring optimal solution feasibility even if storage is present. For a Power-to-Methanol process, we show that DoF reduction should not be applied to all scheduling variables when there is intermediate storage, since it strongly correlates the variables, thus affecting the optimal process design. In a sensitivity analysis concerning the scenario cluster number, we show that scenario clustering based on interpretable features can represent the original space and estimate the objective function with a few scenarios, performing similarly to k-means and k-medoids clustering regarding the objective function. However, despite similar objective values, different optimal designs are identified for different scenario cluster numbers.

1. Introduction

The defossilization of the chemical industry via the substitution of conventional feedstocks and electrification, e.g., through Power-to-X (PtX) processes (Schiffer and Manthiram, 2017; Burre et al., 2020; Mucci et al., 2023b), leads to new challenges for process system design and operation (Mitsos et al., 2018). In particular, flexible operation (Zhang and Grossmann, 2016) of energy-intensive processes like PtX can increase the utilization of renewable sources in both in- and off-grid applications and reduce production costs thanks to the capability of their units to vary their operating point.

In addition to flexible operation, the use of intermediate storage has often been proposed as a way to deal with fluctuations, e.g., in multi-energy systems (Gabrielli et al., 2018), biodiesel production (Wajeh et al., 2024), cryogenic air separation units (Caspari et al., 2019), and PtX such as Power-to-Hydrogen (Mößle et al., 2025), Power-to-Gas (Gorre et al., 2020), Power-to-Ammonia (Allman et al., 2019), and Power-to-Methanol (Svitnič and Sundmacher, 2022; Mucci et al., 2023a). However, flexible operation and storage should be properly evaluated to capture the trade-off between the savings in the operating costs and the additional investment costs for storage and the required oversizing of some process units, while meeting the production goals (Mitsos et al., 2018; Teichgraeber and Brandt, 2020). For this purpose, combined design and scheduling (CDS) optimization problems are generally formulated and solved.

Most works modeling such energy-intensive processes and optimizing their design simultaneously with their scheduling consider exemplary electricity price or renewable power generation profiles. However, the use of different profiles makes the results of these works difficult to compare with each other and generalize. While the use of standardized electricity profiles built from historical data for scheduling problems (Papadimitriou et al., 2025) can overcome the first issue, the challenge of accurately capturing the uncertainty related to scenario realization remains. Two-stage stochastic programming (Mitsos et al., 2018; Conejo et al., 2010; Li and Grossmann, 2021), one of

☆ This article is part of a Special issue entitled: 'Emerging Stars II' published in Chemical Engineering Research and Design.

* Corresponding author at: Department of Chemical Engineering, KU Leuven, 3001 Leuven, Belgium.
E-mail address: dominikbongartz@alum.mit.edu (D. Bongartz).

https://doi.org/10.1016/j.cherd.2025.09.046
Received 24 July 2025; Received in revised form 12 September 2025; Accepted 27 September 2025
Available online 3 October 2025
0263-8762/© 2025 The Authors. Published by Elsevier Ltd on behalf of Institution of Chemical Engineers. This is an open access article under the CC BY license (http://creativecommons.org/licenses/by/4.0/).

the approaches for optimization under uncertainty, can overcome this issue. However, such two-stage stochastic optimization (TSO) problems become computationally challenging to solve both locally and globally, or even unsolvable within a reasonable time, when there are nonlinearities, the number of scenarios increases, and finely time-discretized or relatively long horizons are considered for scheduling.

To tackle the high numerical complexity of such problems, the models are often simplified, e.g., by removing model nonlinearities or integer variables (Raheli et al., 2023), by reformulating them as scheduling-informed design problems (Allman et al., 2019), and by discretizing the original time series for multi-period optimization (Martín, 2016; Maggi et al., 2023). In addition, typical or representative periods can be identified as time slices (Fig. 1), e.g., via heuristics and scenario clustering approaches (Hoffmann et al., 2020), or generated, e.g., via k-means (Hoffmann et al., 2020), to represent the original scenario space with fewer scenarios, thus significantly reducing the size of the original optimization problems. Analogously, the number of optimization variables related to the time steps of each scenario can be reduced via time series aggregation approaches such as downsampling and segmentation (Hoffmann et al., 2020; Bahl et al., 2018). However, such methods do not generally retain time step chronology information, essential for systems with storage, unless the time-related degrees of freedom (DoF) are mapped (Schäfer et al., 2020a) or additional variables and constraints are introduced to account for inter-period storage levels (Hoffmann et al., 2020; Baumgärtner et al., 2019b).

Scenario clustering (Hoffmann et al., 2020) could potentially be performed inside the solver to capture the interplay between the scenario time series and the SO problem (Cao et al., 2016). More commonly though, scenarios are clustered outside the solver and *ex-ante*, i.e., before solving the optimization problems. Several outside-the-solver scenario clustering approaches based on heuristics (Martín, 2016; Maggi et al., 2023; Karuppiah et al., 2010; Belderbos and Delarue, 2015; Poncelet et al., 2017), brute force (De Sisternes and Webster, 2013), hierarchy (Poncelet et al., 2017; Kotzur et al., 2018; Teichgraeber and Brandt, 2019; Pfenninger, 2017; Zhang et al., 2023), correlation loss (Hu and Li, 2019), or different distance definitions such as the forward selection and backward reduction approaches (Conejo et al., 2010; Heitsch and Römisch, 2003; Dupačová et al., 2003; Heitsch and Römisch, 2009; Bruninx and Delarue, 2016), k-means and k-medoids (Kotzur et al., 2018; Teichgraeber and Brandt, 2019; Pfenninger, 2017; Zhang et al., 2023), have been proposed to simplify optimization problems. An overview of the main clustering approaches proposed in literature can be found in Fig. 1.

Some of these scenario clustering approaches have been compared for different applications, e.g., for a risk-averse stochastic problem of a generalized continuous process (Germscheid et al., 2024), generation expansion planning (Poncelet et al., 2017; Almaimouni et al., 2018), stochastic unit commitment (Bruninx and Delarue, 2016; Dvorkin et al., 2014), energy supply systems (Kotzur et al., 2018; Pfenninger, 2017; Helistö et al., 2020; Raya-Tapia et al., 2025), an electricity storage (Teichgraeber and Brandt, 2019) and a gas turbine power generation problem (Teichgraeber and Brandt, 2019). However, based on the results of the above-mentioned works, no clustering approach consistently performs best, as its performance most likely depends on the problem itself.

The above-mentioned clustering approaches generally consider the time series of the original scenario space to determine a pre-defined number of representative scenarios. As an alternative, a set of features extracted from each scenario can be used as input space for the so-called feature-based clustering (Liao, 2005). The sets of features are like scenario fingerprints and are used to identify the corresponding scenarios once clustering is performed. For example, the most relevant eigenvalues of the scenario time series extracted via principal component analysis (PCA) could be used as features for clustering (Almaimouni et al., 2018; Phillips, 2024). Also, interpretable features such as central moments, e.g., mean and standard deviation, can be considered for clustering. Alternatively, information from preliminary optimization runs can be used as features to account for the interplay between the input scenarios and the model itself (Zhang et al., 2023; Phillips, 2024; Sun et al., 2019; Jürgens et al., 2024). However, this type of *ex-post* feature-based clustering, also called decision-based clustering, requires high computational resources compared to other *ex-ante* clustering approaches (Jürgens et al., 2024) and does not always outperform them (Phillips, 2024).

Although feature-based scenario clustering can filter some noise from the scenario time series, namely, underlying data patterns that are not necessary for TSO problems, it is rarely applied in TSO problems (Almaimouni et al., 2018; Phillips, 2024). Further, which features should be considered to generate the scenario fingerprints for clustering is unclear. We therefore address these literature shortcomings by applying feature-based scenario clustering to reduce the numerical complexity of stochastic CDS optimization problems. A Power-to-Methanol (PtMeOH) process with intermediate storage based on our previous work (Mucci et al., 2023a) is considered as a case study. Furthermore, we investigate the use of both interpretable and non-directly interpretable features, i.e., central moments and principal components from PCA, respectively, for scenario clustering, and compare feature-based clustering against k-means and k-medoids, the state-of-the-art clustering approaches.

Also, we combine feature-based scenario clustering with DoF reduction for the scheduling variables to reduce the number of optimization variables further and handle longer time horizons in such TSO problems. In particular, for each instance of the SO problem, we linearly map the scheduling variables from the original to the reduced time domain before solving the stochastic CDS problem, while maintaining the information on the chronology of time steps so that the obtained scheduling is feasible even in the presence of storage. Further, we evaluate how applying DoF reduction *selectively* to the scheduling variables affects the optimal solution; this represents another element of novelty of this work.

The remainder of the article is structured as follows: Section 2 presents the methodology; Section 3 the considered process and case studies, while Sections 4 and 5 the optimization results and the conclusions. Additional modeling assumptions and results are provided within the Appendix A and Supporting Information.

2. Methodology

In stochastic CDS problems (OP1), the weighted sum of the scenario objective functions Obj_n over the N_{scen} scenarios is minimized with respect to first-stage or design ($\boldsymbol{d}$) variables and second-stage or scheduling ($\boldsymbol{s}_n$) variables subject to equality (h_n) and inequality (g_n) constraints. Obj_n, h_n and g_n can depend on the input scenario $\boldsymbol{c}_n \in \mathbb{R}^{N_{\mathrm{TS}}}$ with N_{TS} time steps:

$$\min_{\boldsymbol{d},\boldsymbol{s}} \left(\sum_{n=1}^{N_{\mathrm{scen}}} p_n \cdot \mathrm{Obj}_n(\boldsymbol{d}, \boldsymbol{s}_n(\boldsymbol{c}_n)) \right) \tag{OP1}$$

$$s.t.$$

$$h_n(\boldsymbol{d}, \boldsymbol{s}_n(\boldsymbol{c}_n)) = 0 \qquad n = 1, \dots, N_{\mathrm{scen}}$$

$$g_n(\boldsymbol{d}, \boldsymbol{s}_n(\boldsymbol{c}_n)) \leq 0 \qquad n = 1, \dots, N_{\mathrm{scen}},$$

where $\boldsymbol{p} \in \mathbb{R}^{N_{\mathrm{scen}}}$ are the scenario probabilities, and $\boldsymbol{d} \in \mathbb{R}^{N_{\mathrm{design\ var}}}$ and $\boldsymbol{s} \in \mathbb{R}^{N_{\mathrm{scen}} \times N_{\mathrm{scheduling\ var}} \times N_{\mathrm{TS}}}$ the optimization variables with $N_{\mathrm{design\ var}}$ and $N_{\mathrm{scheduling\ var}}$ being the number of design and scheduling variables, respectively. Also, note that we consider uncertainty between the scenarios, but not between the scenario time steps, i.e., the full sequence of N_{TS} values within each scenario $\boldsymbol{c}_n$ is assumed to be known.

To solve computationally challenging TSO problems with high numbers of scenarios and relatively long time horizons, we combine two strategies: (1) the reduction of the scenario space via clustering and (2) the reduction of DoFs related to the scheduling variables. Note that, in our case, each scenario $\boldsymbol{c}_n$ is a time series with N_{TS} time steps each, and both its size and the number of DoFs scale with the time horizon.

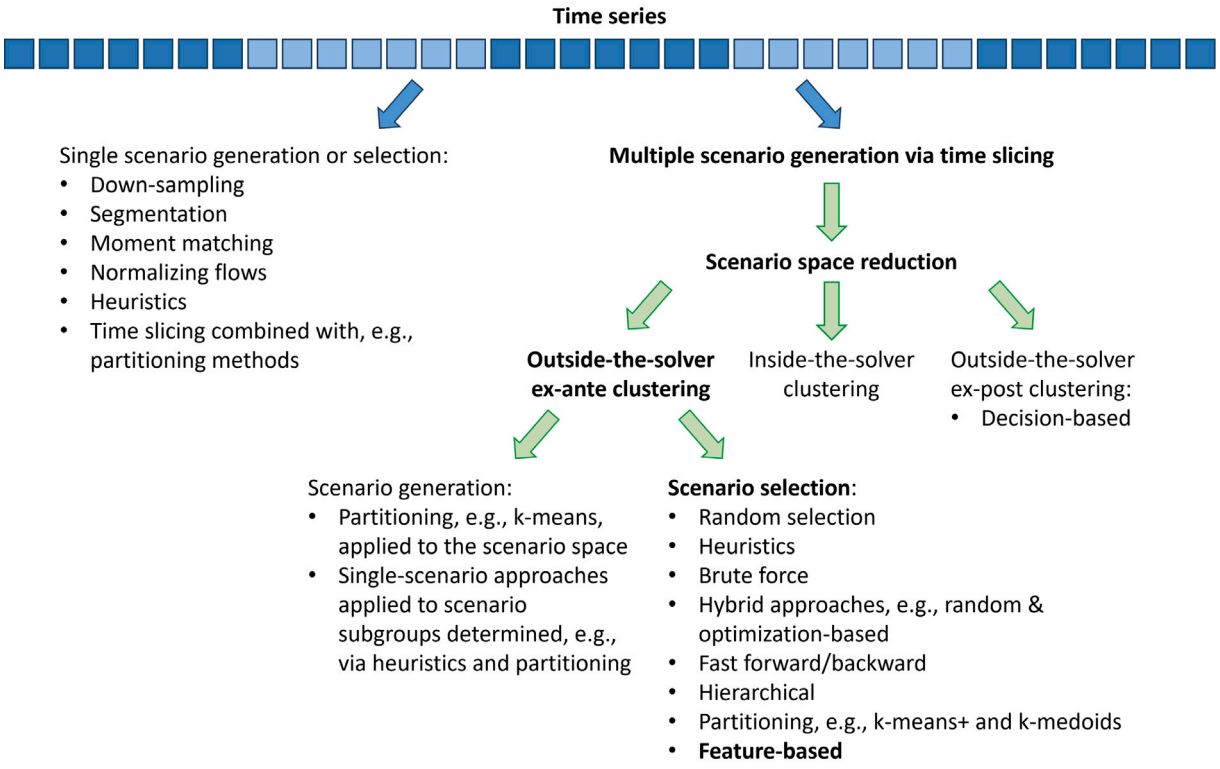


Fig. 1. Overview of the main approaches for either single scenario or reduced scenario space generation from an input time series, which is displayed in blue. The main clustering approach investigated within this work is displayed in bold. Note that, in contrast to *generated* scenarios, *selected* scenarios are data slices that belong to the input time series.

2.1. Scenario clustering

The underlying assumption of scenario clustering is that the optimizer chooses similar process designs for scenarios with similar characteristics. Thus, the scenarios can be grouped into $N_{\text{scen, red}}$ clusters according to their similarities. Then, a representative scenario c_n for each cluster n can be selected (or generated), and its probability $p_{\text{red},n}$ evaluated based on the cluster size: $c \in \mathbb{R}^{N_{\text{scen, red}} \times N_{\text{TS}}}$ and $p_{\text{red}} \in \mathbb{R}^{N_{\text{scen, red}}}$, i.e., the matrix and the vector with all representative scenarios and their probabilities, respectively, are the input of the TSO problem (OP2):

$$\min_{\boldsymbol{d}, \boldsymbol{s}} \left(\sum_{n=1}^{N_{\text{scen, red}}} p_{\text{red},n} \cdot \text{Obj}_n(\boldsymbol{d}, \boldsymbol{s}_n(\boldsymbol{c}_n)) \right) \tag{OP2}$$

$$s.t.$$

$$h_n(\boldsymbol{d}, \boldsymbol{s}_n(\boldsymbol{c}_n)) = 0 \qquad n = 1, \dots, N_{\text{scen, red}}$$

$$g_n(\boldsymbol{d}, \boldsymbol{s}_n(\boldsymbol{c}_n)) \leq 0 \qquad n = 1, \dots, N_{\text{scen, red}},$$

where $\boldsymbol{d} \in \mathbb{R}^{N_{\text{design var}}}$ and $\boldsymbol{s} \in \mathbb{R}^{N_{\text{scen, red}} \times N_{\text{scheduling var}} \times N_{\text{TS}}}$.

To identify the cluster centers and their probability via feature-based clustering, N_{Feature} features are first extracted from the scenarios to generate an input matrix $B \in \mathbb{R}^{N_{\text{Feature}} \times N_{\text{scen}}}$. Then, k-medoids clustering is used to identify the sub-matrices of B, i.e., the clusters, and the cluster centers, which are columns belonging to the sub-matrices of B. The cluster centers, i.e., the scenario features, are used as fingerprints to identify the corresponding scenarios, which represent the input for (OP2) (see the example in Fig. 2 where mean and standard deviation are used as features).

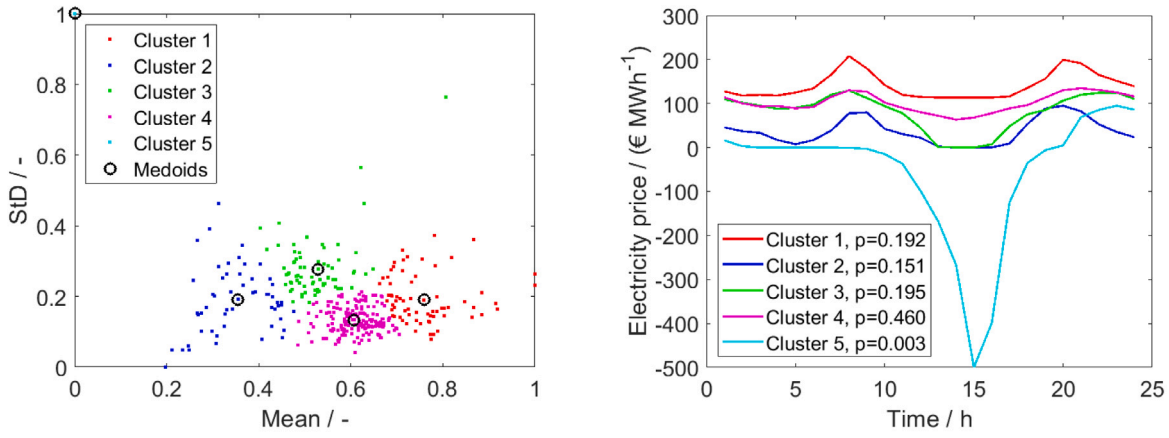
For feature-based scenario clustering, we considered several features: the first four central moments, i.e., mean, standard deviation, skewness, and kurtosis; the mean of the absolute change between consecutive time steps, which can be a significant indicator for storage technologies; and the principal components determined via PCA. Further, the combination of some of these features was also considered. More features would be available for scenario clustering, e.g., features belonging to the spectral domain (Barandas et al., 2020). Nevertheless, we opted for features that are either directly interpretable such as the mean or can be obtained via established data analysis methods, e.g., PCA.

Finally, we benchmarked feature-based clustering against k-medoids and k-means applied directly to the time series of the scenarios, which is the state-of-the-art clustering approach. For an overview of the considered clustering approaches refer to Appendix A.1.

2.2. Degrees of freedom reduction

The underlying assumption of DoF reduction applied to scheduling variables is that the optimizer chooses similar scheduling variable values for similar values of the time-dependent input, e.g., the electricity price. Thus, the input time series can be clustered based on its values, and each scheduling variable is then assigned one DoF for each of these clusters only, instead of one for each of the N_{TS} time steps.

DoF reduction is performed by linearly mapping the scheduling variables from the original time domain to the reduced time domain, thus decreasing the number of distinct scheduling variable values as done, for instance, in Schäfer et al. (2020a) (see an exemplary sketch in Fig. 3). Moreover, this approach maintains memory of the chronological order of time steps and ensures optimal scheduling feasibility in the original time domain, even when storage is present, since the model equality and inequality constraints related to storage can be kept in the original time domain. However, it does impose a restriction compared to the original optimization problem, as it enforces patterns between scheduling variables that can lead to suboptimal (although feasible) solutions of the original problem (Fig. 3).



(a) Feature-based clusters. (b) Scenario cluster profiles.

Fig. 2. Example of feature-based scenario clustering via k-medoids with respect to mean and standard deviation of day-ahead electricity prices for Germany in the year 2023 (ENTSO-E Transparency Platform, 2024). In Figure (a), the normalized mean and standard deviation are shown, where each dot corresponds to a scenario derived from a 24 h time slice of day-ahead electricity prices, as well as the five clusters and cluster medoids. In Figure (b), the day-ahead electricity prices corresponding to the cluster medoids, which represent the reduced scenario space, are shown as well as their probability. (For interpretation of the references to color in this figure legend, the reader is referred to the web version of this article.)

The described DoF reduction via linear mapping can be applied to all scheduling optimization variables. This option significantly reduces the number of optimization variables but, as mentioned above, might affect the optimization results, especially when the scheduling variables do not have a strong dependency on the input time series used for the linear mapping. This case can occur when intermediate decoupling storage is present, since DoF reduction does not account for the intermediate storage level, thus underestimating its utilization potential when performing scheduling. In this work, we therefore also evaluate the option of applying DoF reduction *selectively* to some scheduling variables, thus excluding the remaining ones from the linear mapping.

The optimization problem in the reduced scenario and DoF spaces can be represented as in (OP3):

$$\min_{\boldsymbol{d},\,\tilde{\mathbf{s}}_{\mathrm{dof}}} \left(\sum_{n=1}^{N_{\mathrm{scen,\,red}}} p_{\mathrm{red},n} \cdot \mathrm{Obj}_n(\boldsymbol{d},\, \boldsymbol{s}_n(\boldsymbol{c}_n)) \right)$$

s.t. (OP3)

$$\begin{aligned} &\boldsymbol{s}_n(\boldsymbol{c}_n) = A_{\mathrm{dof},n} \cdot \tilde{\mathbf{s}}_{\mathrm{dof},n}(\boldsymbol{c}_n) && n = 1, \ldots, N_{\mathrm{scen,\,red}} \\ &h_n(\boldsymbol{d},\, \boldsymbol{s}_n(\boldsymbol{c}_n)) = 0 && n = 1, \ldots, N_{\mathrm{scen,\,red}} \\ &g_n(\boldsymbol{d},\, \boldsymbol{s}_n(\boldsymbol{c}_n)) \le 0 && n = 1, \ldots, N_{\mathrm{scen,\,red}}, \end{aligned}$$

where $\boldsymbol{d} \in \mathbb{R}^{N_{\mathrm{design\,var}}}$, $\boldsymbol{s} \in \mathbb{R}^{N_{\mathrm{scen,\,red}} \times N_{\mathrm{scheduling\,var}} \times N_{\mathrm{TS}}}$, $\tilde{\mathbf{s}}_{\mathrm{dof}} \in \mathbb{R}^{N_{\mathrm{scen,\,red}} \times N_{\mathrm{scheduling\,var}} \times N_{\mathrm{dof,\,sched}}}$, and $N_{\mathrm{dof,\,sched}}$ is the number of DoFs per scheduling variable, which is chosen to be much smaller than N_{TS}. The scheduling variables $\boldsymbol{s}_n$ are linearly mapped to the scheduling variables in the reduced DoF space $\tilde{\mathbf{s}}_{\mathrm{dof},n}$ via the matrix $A_{\mathrm{dof},n}$. Note that, when DoF reduction is performed selectively, the linear mapping of the scheduling variables is applied only to some of the $N_{\mathrm{scheduling\,var}}$ distinct scheduling variables.

After implementing and testing several equivalent model formulations to embed DOF reduction (see Section 1 of Supporting Information), we opted for a reduced-space formulation (Bongartz and Mitsos, 2017). In this way, we not only reduce the number of DoFs via the linear mapping as equality constraints but also explicitly eliminate $\boldsymbol{s}_n$ via this mapping. This approach reduces the number of variables and constraints in the optimization problem, and thus its size. This can potentially reduce the computational time of solvers for large optimization problems.

DoF reduction is applied to the scheduling variables of each scenario cluster c_n independently. To determine the linear mapping matrix A_{dof}, we apply k-medoids to the normalized input scenario time series. Further, we tested two approaches for generating the linear mapping matrix A_{dof}: using k-medoids including and excluding the extreme values of the input time series. In the latter case, we assigned two DoFs to the lowest and highest values of the original time series, and then created $N_{\mathrm{dof,\,sched}} - 2$ clusters via k-medoids with the remaining values of the input time series. This choice is motivated by the fact that a few extreme hours can significantly affect the representativeness of the reduced time series (Teichgraeber and Brandt, 2020; Kotzur et al., 2018; Teichgraeber et al., 2020; Merrick, 2016) and a special handling of those might be beneficial.

Finally, although the best number of DoFs could be determined while optimizing, e.g., by applying wavelet grid adaptation (Schäfer et al., 2020a,b; Papadimitriou et al., 2023), we chose the number of DoFs after preliminary analyses to avoid introducing an iterative loop with TSO problems to solve.

2.3. Implementation

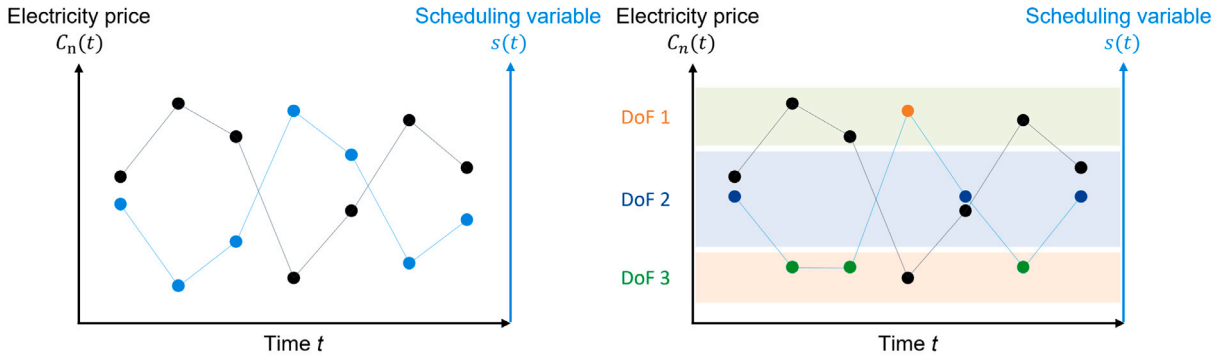
The above-described methodology and the two-stage stochastic optimization problems were implemented and solved in Matlab and GAMS. In particular, data processing, scenario clustering, and DoF reduction were performed in Matlab *ex-ante*, while the deterministic equivalent of the TSO problems was implemented in GAMS and solved with the global optimizer BARON 23.6.22 (Khajavirad and Sahinidis, 2018).

The information about the scenario clusters and the linear mapping matrix was passed from Matlab to GAMS through GAMS data exchange files (.gdx files) and Excel data sheets. Further, GAMS was called directly from MATLAB to solve the optimization problems, thus making it possible to embed the optimization problems in iterative loops, e.g., for a sensitivity analysis with respect to the number of scenario clusters. A CPU time limit of 4 h and 12 h was imposed for the optimization runs with a daily and weekly scheduling horizon, respectively.

The code is made available in the Supporting Information for the implementation details.

3. Case studies

The above-described methodology was applied to the deterministic equivalent of a TSO problem that simultaneously optimizes the design and scheduling of a PtMeOH process with intermediate storage.



(a) No DoF reduction. (b) With DoF reduction.

Fig. 3. Exemplary sketch of DoF reduction that conserves time step chronology. In Figure (a), where no DoF reduction is performed, the scheduling variable $s(t)$ can have a different value at every time step. In Figure (b), the input time series values, i.e., the electricity prices $C_{EP}(t)$, were assigned to three groups (indicated with the shaded areas), and the scheduling variable $s(t)$ are constrained to have the same value for each time step in which the input values belong to the same group. However, the value of the scheduling variable for each group can be optimized. Thus, there are three DoFs in this example.
Note: The groups in the input time series value range and the corresponding scheduling variable value are displayed in the same color. (For interpretation of the references to color in this figure legend, the reader is referred to the web version of this article.)

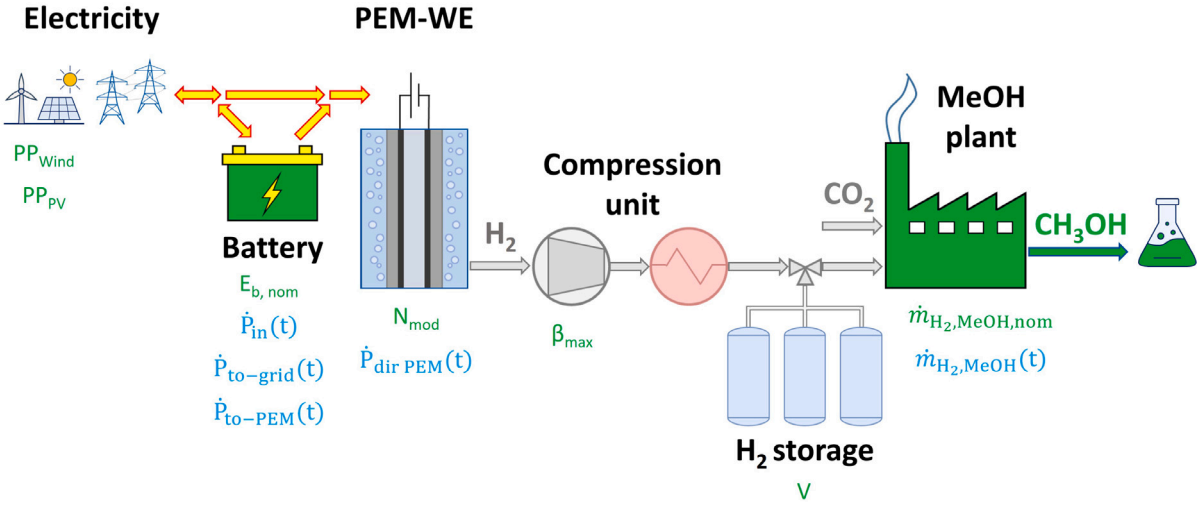


Fig. 4. Sketch of the Power-to-Methanol process considered for the stochastic CDS problems. The design and scheduling optimization variables are displayed in green and light blue, respectively. Note that the sizes of the renewable power plant (PP_{Wind} and PP_{PV}) are optimization variables only for the stand-alone case study. Also, the power that is supplied back to the grid ($P_{to-grid}(t)$) is an optimization variable only for the grid-connected case study. Refer to Table 1 for more details on the optimization variables. (For interpretation of the references to color in this figure legend, the reader is referred to the web version of this article.)

The considered PtMeOH process is composed of five units, namely, a battery, a PEM water electrolysis (PEMWE) unit, a mechanical hydrogen compression unit, a pressurized vessel for hydrogen storage, and a methanol synthesis plant (Fig. 4). In particular, the PEMWE unit produces hydrogen, which is then compressed in a two-stage mechanical compressor before being fed into the pressurized hydrogen vessel. A certain hydrogen flow rate is taken from the vessel and then combined with a stoichiometric CO_2 flow rate to synthesize methanol. Additionally, the battery can store energy when electricity prices are favorable or there is a surplus of renewable power in the grid-connected and stand-alone case study, respectively. The energy stored in the battery will be provided at a later time either to the PtMeOH plant or the grid depending on the case study and the economics.

The process model is an MINLP to account for the operating limits and nonlinearities of the process unit efficiency and energy demand as well as the cost correlations. Also, the model is quasi-steady state due to the relatively fast dynamics of the key process units (Mucci et al., 2023b; Kopp et al., 2017; BSE engineering, 2025) compared to the considered time step (1 h), and is taken from our previous work (Mucci et al., 2023a). Furthermore, we assume a maximum hourly ramp rate of 10% for the methanol synthesis plant, which is lower than typical capabilities (BSE engineering, 2025), since moderate flexibility already provides most of the economic benefits (Mucci et al., 2023a). A few modifications to the PtMeOH model (Mucci et al., 2023a) were made to reduce the number of intermediate variables and update the unit investment costs with respect to inflation to the year 2023 (see Appendix A.2 for additional details).

The input scenario space for the TSO problems was obtained by slicing a one-year input time series of electricity prices and renewable power generation for Germany from 2023, thus being consistent with the considered economic data. In particular, daily and weekly scenarios with hourly resolution were extracted from the input time series. For weekly scenarios, 359 profiles composed of seven consecutive days were obtained by slicing the yearly time series and shifting the starting day. This choice increases the possibilities of the scenario clustering algorithm to determine representative profiles, since the scenarios do not necessarily start on the same day of the week.

The chosen time horizons enable evaluating storage utilization benefits, as the profiles capture significant profile variations, e.g., between

$$\mathrm{LCOM} = \sum_{n=1}^{N_{\mathrm{scen,red}}} p_{\mathrm{red},n} \cdot \mathrm{LCOM}_n(\boldsymbol{d}, \boldsymbol{s}_n) = \sum_{n=1}^{N_{\mathrm{scen,red}}} p_{\mathrm{red},n} \cdot \frac{\mathrm{CAPEX}_0(\boldsymbol{d}) + \mathrm{CAPEX}_{\mathrm{r,PEM}}(\boldsymbol{d}) \cdot (1+i)^{-10} + \sum_{j=1}^{N_y} (\mathrm{O\&M}(\boldsymbol{d}) + \mathrm{OPEX}_{y,n}(\boldsymbol{d}, \boldsymbol{s}_n)) \cdot (1+i)^{-j}}{\sum_{j=1}^{N_y} (M_{\mathrm{MeOH,y}}) \cdot (1+i)^{-j}}$$

Box I.

working days and weekends for the electricity price, and assessing whether investing in large capacity storage instead of small capacity storage is worth it. Although even longer time horizons could provide more insights, we did not consider them because we target a methanol process with a nearly continuous demand throughout the year, e.g., to serve a downstream process. Additionally, it would have increased numerical complexity and weakened the assumption of perfect knowledge of scenario time step sequences, since long-term profile predictions suffer from poor reliability.

Further, solving TSO problems for other input scenario data, e.g., considering several years (Poncelet et al., 2017; Pfenninger, 2017), could potentially increase the confidence in the obtained optimal process designs. However, the input scenario sets remain uncertain, since there is no guarantee that the considered scenarios will actually occur in the future. Therefore, this type of analysis is out of scope of this work.

In the following subsections, we provide additional details on the two considered case studies: a grid-connected and a stand-alone PtMeOH process.

3.1. Grid-connected Power-to-Methanol process

Concerning the design, the nominal sizes of the battery, PEM water electrolyzer, compression unit, hydrogen storage, and methanol synthesis plant, which is defined in terms of the nominal hydrogen flow rate, are optimized. Note that the pressure of the PEM water electrolyzer is not a design variable but is set to 40 bar differently from our previous work (Mucci et al., 2023a). Concerning the scheduling, the power flows in the battery and PEM water electrolyzer as well as the hydrogen outlet flow rate from the hydrogen storage are optimized. The considered optimization variables can be found in Table 1 and are displayed in Fig. 4.

The objective function considered is the levelized cost of methanol (LCOM) (see the equation in Box I), where CAPEX_0 is the initial investment cost, O&M the operation and maintenance costs, $\mathrm{OPEX}_{y,n}$ the yearly operating costs for the scenario c_n, and N_y the plant lifetime. The investment cost for replacing the electrolysis unit ($\mathrm{CAPEX}_{\mathrm{r,PEM}}$) is also considered. Thus, the objective function captures the trade-off between the investment and O&M costs, which depend on the design variables, and the weighted sum of the yearly operating costs, which depend on both design and scheduling variables. The operating costs calculated via the scheduling over the considered time horizon are then proportionally scaled to meet the number of yearly operating weeks (48 w/y).

We neglected the additional costs related to electricity taxes and grid balancing, which can be significant (BDEW Bundesverband der Energie- und Wasserwirtschaft, 2025) but are generally location-dependent. Thus, the calculated levelized cost of methanol represents an underestimation of the production price.

Differently from our previous work (Mucci et al., 2023a) where the yearly methanol production rate ($M_{\mathrm{MeOH,y}}$) was the result of the optimal process scheduling, a yearly production goal of 50 kt is considered to ease comparability between process designs obtained with different clustering approaches and to reduce the nonlinearities of the objective function. Therefore, the denominator of the objective function does not depend on any optimization variables. The production goal is enforced via an inequality constraint to reduce the numerical complexity via relaxation. This simplification is possible since we assume that as much power as needed can always be taken from the grid.

When considering daily scenarios, the scheduling variables were kept in the original time domain, thus avoiding suboptimal solutions of the original problem, since it could be handled numerically. In contrast, when considering weekly scenarios, DoF reduction for the scheduling variables was performed to reduce the numerical complexity (see Section 2.2). In particular, we applied k-medoids clustering to the electricity price scenarios of the reduced scenario space to determine the linear mapping matrix.

3.2. Stand-alone Power-to-Methanol process

In addition to the design variables considered for the grid-connected case study, the size of a PV and wind power plant is optimized. Concerning the scheduling, the power flows in the battery and PEM water electrolyzer as well as the hydrogen outlet flow from the hydrogen storage are optimized. In addition, renewable curtailment is considered as it can reduce the production cost in stand-alone plants (Svitnič and Sundmacher, 2022; Mucci et al., 2023a). The considered optimization variables can be found in Table 1 and are displayed in Fig. 4.

The stand-alone PtMeOH process is also optimized with respect to the levelized cost of methanol. In contrast to the grid-connected case study, however, no yearly production target was enforced for each scenario since the methanol production depends on the renewable power availability of the scenario. In fact, a big renewable power plant would be needed to meet a certain production target for scenarios with low capacity factors of the renewable power plant, while the same plant design would be either infeasible or highly oversized for scenarios with high capacity factors. Therefore, an average production target over the considered scenarios was set:

$$M_{\mathrm{MeOH,y}} = \sum_{n=1}^{N_{\mathrm{scen,red}}} p_{\mathrm{red},n} \cdot M_{\mathrm{MeOH,y},n}(\boldsymbol{d}, \boldsymbol{s}_n) \in [50, 55\ \mathrm{kt}].$$

Additionally, a minimum yearly production rate of 5 kt was set for every scenario.

In analogy to the grid-connected case study, we performed DoF reduction only for the weekly scenarios by applying k-medoids to the weekly renewable power generation scenarios. Note that a guess on the size of the renewable power plants (design variables $\mathrm{PP}_{\mathrm{PV}}$ and $\mathrm{PP}_{\mathrm{Wind}}$), e.g., from preliminary optimization runs, is needed to obtain the renewable power generation profile for every scenario prior performing DoF reduction, since this profile depends on the share of solar vs. wind power. Moreover, when performing a sensitivity analysis with respect to the number of scenario clusters, the optimal values from the previous optimization run with a lower number of scenario clusters were assumed as initial guesses (the optimal $\mathrm{PP}_{\mathrm{PV}}$ and $\mathrm{PP}_{\mathrm{Wind}}$ from the sensitivity analysis in Section 4.2.1 were assumed as a guess for the optimization with the lowest value of scenario clusters). This choice allows considering up-to-date information for clustering, but can introduce approximation errors in the case such design variables ($\mathrm{PP}_{\mathrm{PV}}$ and $\mathrm{PP}_{\mathrm{Wind}}$) change their value significantly with respect to the scenario cluster number.

Table 1
Design and scheduling variables of the optimization problem for the grid-connected and stand-alone case studies with their upper and lower bounds.

Unit	Symbol	Description of the design variable	Lower bound	Upper bound
PV plant[a]	PP_{PV}	Nominal power peak of the PV power plant	50 MW	250 MW
Wind plant[a]	PP_{Wind}	Nominal power peak of the wind power plant	100 MW	300 MW
Battery	$E_{b,nom}$	Energy capacity	5 MWh	150 MWh
PEM-WE	N_{mod}	Number of electrolysis modules	25	40
H_2 compression	β_{max}	Maximum pressure ratio	1.88	3.50
H_2 storage	V	Volume of the vessel	50 m^3	1500 m^3
MeOH plant	$\dot{m}_{H_{2,MeOH,nom}}$	Nominal H_2 flow rate for the methanol synthesis plant	1.2 t/h	1.8 t/h
Unit	**Symbol**	**Description of the scheduling variable**	**Lower bound**	**Upper bound**
Battery	$P_{in}(t)$	Power input	0.5 MW[b]	$\min(100\ MW, (0.9 \cdot E_{b,nom/1h}))$
	$P_{to-grid}(t)$	Power output, electricity back to the grid (AC)	0.5 MW[b]	$\min(100\ MW, (0.9 \cdot E_{b,nom/1h}))$
	$P_{to-PEM}(t)$	Power output, electricity to the electrolyzer	0.5 MW[b]	$\min(100\ MW, (0.9 \cdot E_{b,nom}/1h))$
PEM-WE	$P_{dir\ PEM}(t)$	Power directly from the grid/renewable plant	0.5 MW $\cdot N_{mod}$[b]	2.5 MW $\cdot N_{mod}$
H_2 storage	$\dot{m}_{H_{2,MeOH}}(t)$	H_2 flow rate from storage to the methanol synthesis plant	$0.2 \cdot \dot{m}_{H_{2,MeOH},nom}$	$\dot{m}_{H_{2,MeOH,nom}}$

[a] Design variable considered in the stand-alone Power-to-Methanol case study only.
[b] 0 MW if the unit is not operating - enforced via binary variables (not shown).

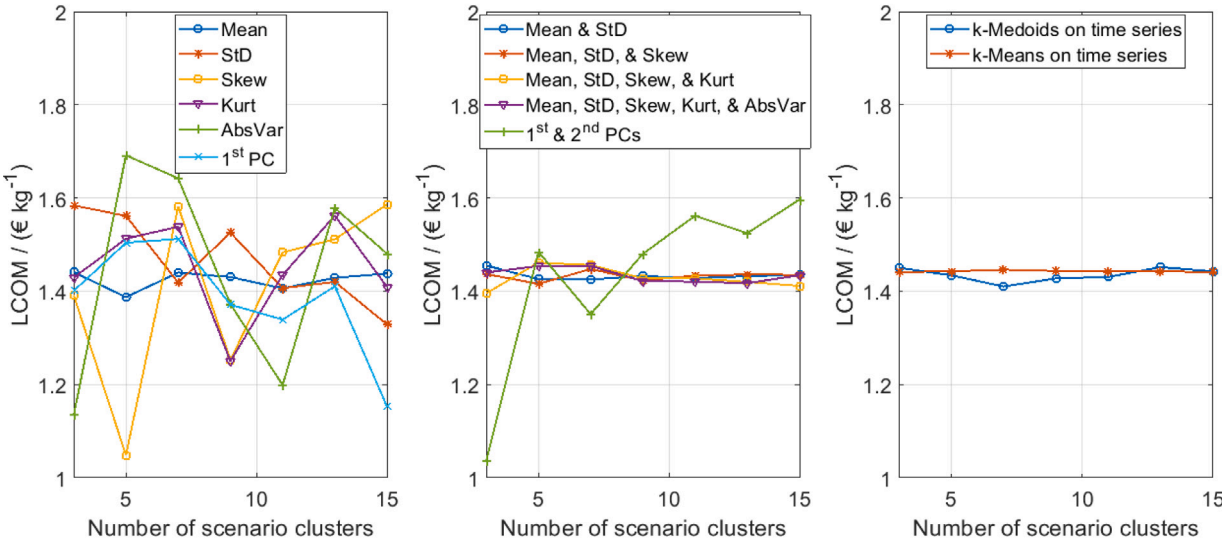


Fig. 5. Levelized cost of methanol (LCOM) for the grid-connected case study for different numbers of daily scenario clusters and clustering approaches. Left: Single-feature clustering via k-medoids based on mean, standard deviation (StD), skewness (Skew), kurtosis (Kurt), the mean of the absolute variation between consecutive time steps (AbsVar), and principal components (PCs). Middle: Multi-feature clustering via k-medoids based on the previously mentioned features. Right: k-medoids and k-means applied to the original time series.

4. Results and discussion

In the following, Sections 4.1 and 4.2 compare the clustering approaches for daily and weekly scenarios, respectively. Moreover, the latter investigates the effect of applying DoF reduction selectively to some scheduling variables. Finally, the results are discussed in Section 4.3.

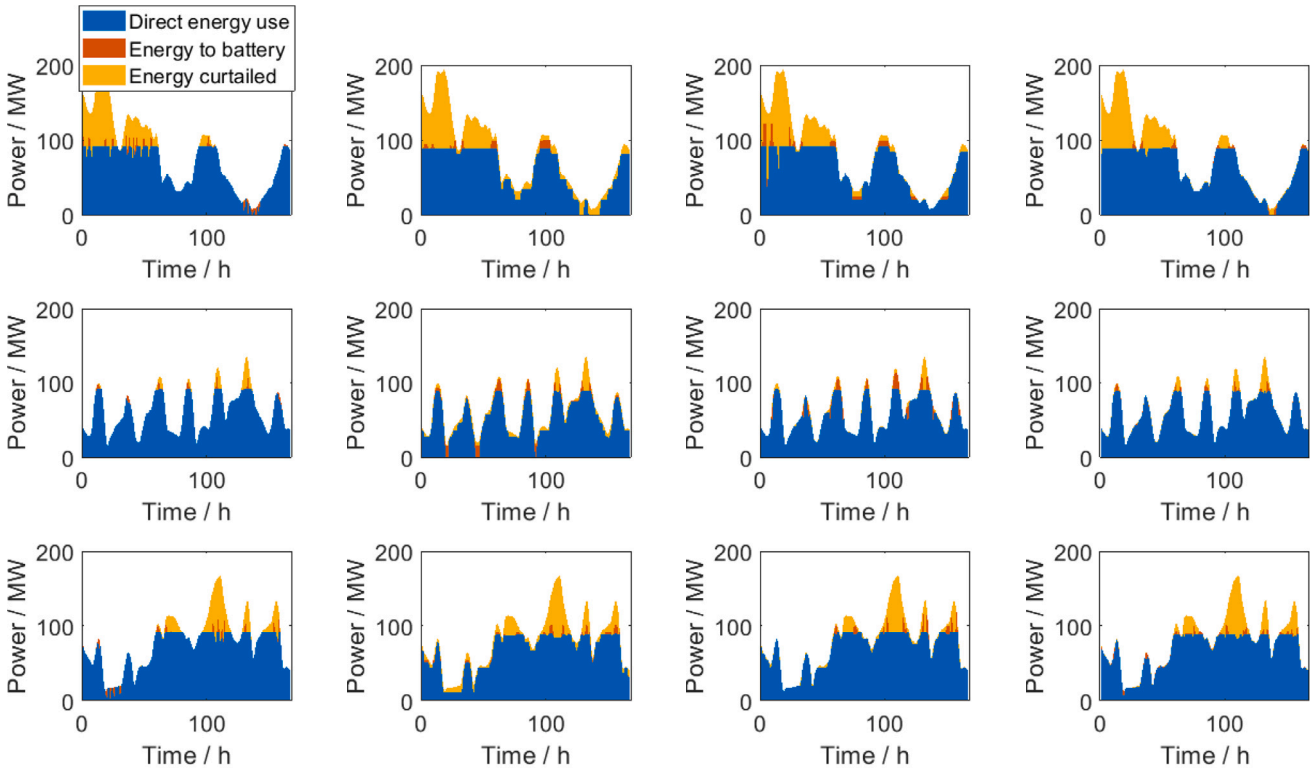
4.1. Daily scenarios: Effect of clustering approaches and number of scenario clusters

In this subsection, we compare the considered feature-based scenario clustering approaches (see Table A.1) for a different number of daily scenario clusters ($N_{scen,red}$) with hourly resolution for the grid-connected Power-to-Methanol process. $N_{scen,red}$ was varied since the number of scenario clusters needed to represent the original scenario space properly is not known in advance. Also, we considered a daily scenario horizon to maintain an acceptable numerical complexity, thus avoiding suboptimal solutions due to DoF reduction and isolating the effect of the scenario clustering approach and $N_{scen,red}$ on the objective function (Fig. 5).

When the scenarios are clustered based on a single feature, the objective function varies quite significantly with respect to the number of scenario clusters. This means that single-feature scenario clustering is not able to identify representative scenario subsets and probabilities for low $N_{scen,red}$. Among the considered features, the mean value of the scenario time series provides an objective function that is the least dependent on $N_{scen,red}$. This result suggests that the mean is the most relevant feature to estimate the production cost. This result was expected since the average electricity price (and renewable power availability for a stand-alone case study) directly affects the operating costs.

When several features are simultaneously considered for clustering, the objective function remains nearly constant with respect to $N_{scen,red}$, thus meaning that a limited amount of clusters, e.g., nine (<3% of the original scenario space), is sufficient to estimate the LCOM for the considered case study. Further, multi-feature clustering always outperforms single-feature clustering, since the objective function is less dependent on $N_{scen,red}$; thus, the latter has not been considered when investigating longer time horizons in Section 4.2.2.

No major differences can be noticed between the multi-feature clustering approaches, except for the one using the first two principal components extracted from the original scenario time series. Thus, the most relevant eigenvalues calculated from the input time series seem to be less important than other features, e.g., the central moments, to estimate the methanol production cost with low $N_{scen,red}$.



(a) No DoF reduction.

(b) $N_{\text{dof, sched}} = 12$, all scheduling variables mapped.

(c) $N_{\text{dof, sched}} = 12$, $P_{\text{dir PEM}}(t)$ and $P_{\text{in}}(t)$ mapped.

(d) $N_{\text{dof, sched}} = 48$, all scheduling variables mapped except for $\dot{m}_{\text{H}_{2,\text{MeOH}}}(t)$.

Fig. 6. Optimal solution of the two-stage stochastic problem for a stand-alone Power-to-Methanol plant when considering three weekly scenario clusters (the three rows) and different time series aggregation strategies, i.e., no DoF reduction (Figure (a)), 12 DoFs where all scheduling variables are mapped (Figure (b)), 12 DoFs where only $P_{\text{dir PEM}}(t)$ and $P_{\text{in}}(t)$ are mapped (Figure (c)), and 48 DoFs where all scheduling variables except for $\dot{m}_{\text{H}_{2,\text{MeOH}}}(t)$ are mapped. The renewable energy that is directly used in the Power-to-Methanol plant, the energy stored in the battery, and the curtailed renewable energy are displayed. The figure shows that either DoF reduction applied to a few scheduling variables with a relatively low number of DoFs (Figure (c)) or DoF reduction applied to most scheduling variables with a higher number of DoFs (Figure (d)) is necessary to properly match the optimal solution of the problem where no DoF reduction is performed. (For interpretation of the references to color in this figure legend, the reader is referred to the web version of this article.)

When the input time series are directly clustered (k-means and k-medoids approaches), the objective function value is nearly independent with respect to the scenario cluster number, similarly to the results obtained with multi-feature clustering. Moreover, these objective function values are similar to the ones obtained with multi-feature clustering.

For the sake of completeness, we report the results of the optimal design variables as well as the results of the same analysis conducted for the stand-alone case study, which has similar outcomes, in Section 3 of Supporting Information.

4.2. Weekly scenarios

Differently from the TSO problems solved for daily scenarios (Section 4.1), we apply DoF reduction to reduce the optimization problem sizes related to the longer time horizon considered in this subsection, i.e., a week. Therefore, this subsection first investigates selective DoF reduction as a trade-off between numerical complexity and solution accuracy, and then compares the clustering approaches for different numbers of scenario clusters.

4.2.1. Degrees of freedom reduction

In the following, we present the results of DoF reduction for the stand-alone PtMeOH case study with three weekly scenarios identified via multi-feature clustering based on the first four central moments. Note that the chosen clustering approach does not significantly affect the choice of the number of DoFs since the same input profiles are considered for all cases. Moreover, the power generation profiles were taken from the optimization problem with three scenario clusters solved without applying DoF reduction (Fig. 6(a)). This simpler problem was chosen to be able to compare the results of DoF reduction to the exact solution.

The results in Table 2 show that a relatively high number of DoFs is needed to properly estimate the objective function of the optimization problem in the original time domain: around 24 DoFs for each scheduling variable to achieve an objective function value difference below 2%. In fact, when only a few DoFs are considered, a relevant amount of energy is curtailed, since the power consumption profile does not properly follow the renewable availability profile as shown in Fig. 6(b). This is mainly due to the model constraint that enforces an energy consumption either equal to or lower than the generated energy summed with the energy taken from the battery at every time step. In contrast, a significantly lower DoF number is sufficient to estimate the objective function of the optimization problem in the original time domain for the grid-connected case study, which can always take enough power from the grid, as shown in Appendix A.3.

Concerning the different ways of assigning DoFs, Table 2 shows that assigning DoFs to the extreme values of the input time series to generate the linear mapping is not beneficial for the considered case study, i.e., it leads to a higher LCOM. This might be due to the relatively

Table 2
Comparison of the objective function and the design variable values for different DoF reduction approaches applied to a two-stage stochastic problem of a stand-alone Power-to-Methanol process with intermediate storage. Three renewable power scenario clusters of 168 h each are considered. The number of model variables as well as the NL_{code}, a GAMS indicator of the complexity for handling model nonlinearities, are also displayed. The results were extracted after 6 h CPU time. No global optimality was achieved.

$N_{dof,\,sched}$	Mapped scheduling variables	Specific cost of MeOH	Average MeOH production	En_{batt}	V	N_{mod}	β_{max}	$\dot{m}_{H_{2,MeOH,nom}}$	Model variables	NL_{code}
–		€/kg	kt/y	MWh	m^3	–	–	t/h	–	–
168	None	1.36	50	20	350	34	3.1	1.60	9097	36 433
12	All variables	1.55	47	132	1157	33	3.5[a]	1.90[a]	3481	16 309
12	[b]All variables except for $\dot{m}_{H_{2,MeOH}}(t)$	1.61	43	92	1100	31	3.5[a]	1.40	4417	16 309
12	All variables except for $\dot{m}_{H_{2,MeOH}}(t)$	1.54	48	135	1280	34	3.5[a]	1.51	4417	16 309
12	$P_{dir\,PEM}(t)$ and $P_{in}(t)$	1.42	50	102	250	34	2.5	1.62	7225	33 625
24	All variables	1.43	49	13	1480	35	3.5[a]	1.90[a]	3913	17 857
24	All variables except for $\dot{m}_{H_{2,MeOH}}(t)$	1.40	50	42	680	35	3.5[a]	1.61	4777	17 857
24	$P_{dir\,PEM}(t)$ and $P_{in}(t)$	1.38	51	36	480	35	3.5[a]	1.63	7369	33 841
36	All variables except for $\dot{m}_{H_{2,MeOH}}(t)$	1.39	50	19	930	36	3.5[a]	1.63	5137	19 405
36	$P_{dir\,PEM}(t)$ and $P_{in}(t)$	1.38	50	17	750	35	3.5[a]	1.61	7513	34 057
48	All variables except for $\dot{m}_{H_{2,MeOH}}(t)$	1.38	49	26	455	33	3.5[a]	1.54	5497	20 953
48	$P_{dir\,PEM}(t)$ and $P_{in}(t)$	1.38	51	23	710	36	3.5[a]	1.65	7657	34 273

[a] At bound.
[b] The extremes have a dedicated DoF.

long scenario duration and the input time series: the longer the time horizon, the higher the chances that several peaks or valleys assume similar values (see for instance the power profile in the second row of Fig. 6). Therefore, two DoFs would probably be assigned to these peaks and valleys instead of one if the extremes are handled differently. This can affect the solution, especially when few DoFs are considered. Thus, this option has not been considered for the results shown in Section 4.2.2.

Concerning the possibility of assigning DoF selectively to the scheduling variables, Table 2 shows that the objective function and optimal designs significantly differ for the same number of DoFs. In particular, the fewer scheduling variables are mapped through DoF reduction, the lower the objective function and the closer the optimal design to the design of the benchmark case, i.e., without DoF reduction. This is mainly because the mapping introduces a strong correlation between scheduling variables. However, this correlation might not hold when the scheduling variables do not directly depend on the input time series used for clustering, i.e., the power generation profile, and there is intermediate storage. In fact, the linear mapping is performed without including any information on the storage level, which might affect the optimal process design. Therefore, performing selective DoF reduction, e.g., excluding the scheduling variables that are directly connected to a storage technology (Fig. 6(c) and (d)), provides better solutions while still significantly reducing the numerical complexity (Table 2).

Applying DoF reduction only to the power provided to the battery ($P_{in}(t)$) and to the PEM water electrolyzer ($P_{dir\,PEM}(t)$) shows better results compared to the case where all scheduling variables besides $\dot{m}_{H_{2,MeOH},nom}$ are mapped (Fig. 6(d)). Nevertheless, this leads to a higher numerical complexity when comparing the number of optimization variables and the number of instructions to handle nonlinearities: +28% of optimization variables and +39% NL_{code} increase for an improvement of the objective function lower than 1% (see results for $N_{dof,\,sched} = 48$ in Table 2). Thus, a number of degrees of freedom of 48 and the mapping of all scheduling variables besides $\dot{m}_{H_{2,MeOH},nom}$ represent a good trade-off between number of optimization variables (−40%) and model accuracy (difference in the objective function value lower than 2% compared to the case where no DoF reduction is applied).

4.2.2. Effect of clustering approaches and number of scenario clusters

In the following, we compare the optimization results of the stochastic CDS problems solved with different scenario clustering approaches for different weekly scenario cluster numbers and applying selective DoF reduction for both case studies. In particular, we evaluate the effect of clustering on the objective function and design variables.

To evaluate whether the clustering approaches can identify representative scenario subsets and weights and estimate the objective function value of the full TSO problem, which itself is computationally intractable, we solved a relaxed TSO problem for the full scenario space without DoF reduction using the local optimizer SNOPT 7.7.7 (see Section 2 in Supporting Information for details on the model). Unfortunately, an optimal solution of the relaxed problem, which is an under-estimation of the original problem, was obtained only for the grid-connected PtMeOH case study; for the stand-alone case study, the optimizer did not identify a feasible solution within a CPU time of 3 days.

4.2.2.1. Grid-connected Power-to-Methanol process.

Objective function

In Fig. 7, we show how the objective function evaluated on the reduced scenario space varies with respect to the number of scenario clusters for different clustering approaches.

When multiple interpretable features, namely central moments, are considered for clustering, the levelized cost of methanol (LCOM) is almost independent of the number of clusters in the considered range, thus meaning that a limited number of representative scenarios, e.g., five (ca. 2% of the original scenario space), is sufficient to estimate the objective function value for this case study. In contrast, the objective function shows a strong dependency on $N_{scen,\,red}$ when multi-feature clustering is performed with the first two principal components of the scenarios. In this case, the objective function varies significantly even with relatively high $N_{scen,\,red}$ (this behavior was already observed for daily scenarios as shown in Fig. 5). Moreover, the objective function value is on average significantly lower than the one obtained for the other clustering approaches, thus meaning that this clustering approach does not identify suitable scenario subsets and probabilities to estimate the objective function for the considered case study and $N_{scen,\,red}$ range.

The LCOM obtained with scenarios clustered via k-medoids and k-means applied to the input time series shows the least dependent behavior with respect to $N_{scen,\,red}$ among all the clustering approaches. Nevertheless, the LCOMs obtained via multi-feature clustering are similar to these, thus suggesting that feature-based clustering can identify representative scenario subsets and scenario probabilities. Furthermore, the LCOMs obtained via multi-feature clustering are closer to the LCOM

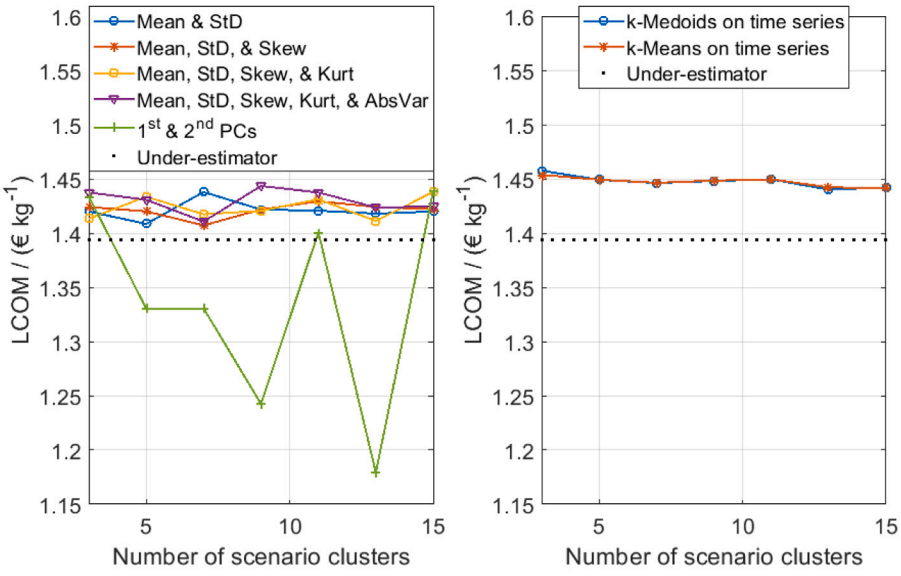


Fig. 7. Levelized cost of methanol for the grid-connected case study for different numbers of weekly scenario clusters and clustering approaches. Left: Multi-feature clustering via k-medoids based on mean, standard deviation (StD), skewness (Skew), kurtosis (Kurt), the mean of the absolute variation between consecutive time steps (AbsVar), and principal components (PCs). Right: k-medoids and k-means clustering applied to the original scenario time series. Weekly scheduling horizons and DoF reduction ($N_{\text{dof, sched}} = 18$) are applied. The black dotted line represents the under-estimator of the original two-stage stochastic problem.

obtained by solving the relaxed TSO problem, thus being closer to the best estimation available of the objective function of the original TSO problem (see Fig. 7).

Design variables

Despite an objective function that is nearly independent of $N_{\text{scen, red}}$, the design variables still exhibit mild variations when increasing the number of scenario clusters for all clustering approaches (see, for instance, the hydrogen flow rate to the methanol synthesis plant in Fig. 9). This behavior was already observed, for instance, by Teichgraeber and Brandt (2020) and can be due to several reasons: approximations due to scenario clustering and DoF reduction; the lack of global convergence; and the fact that several plant designs can have similar objective function values. The latter can be confirmed by fixing the process designs obtained by solving the reduced stochastic CDS problems and then solving stochastic scheduling problems in the original scenario and DoF spaces (Fig. 8). For further analysis on the relationship between design variables and objective function in the original scenario and DoF spaces, we refer to Mucci and Bongartz (2025).

The variations of the design variables with respect to $N_{\text{scen, red}}$ are lower when multi-feature clustering instead of k-medoids and k-means applied directly to the input time series is performed and a sufficiently high number of clusters is considered (see, for instance, Fig. 10). Furthermore, these variables are on average less dependent on $N_{\text{scen, red}}$ when it is higher, e.g., than nine, and their values are quite similar across the multi-feature clustering approaches. Moreover, the process designs identified via multi-feature clustering (and selective DoF reduction) perform on average slightly better for the considered case study (Fig. 8). This suggests that the proposed methodology generates reduced S-CDS problems that preserve the key characteristics of the original S-CDS problem, thus allowing identifying promising design candidates.

Similarly to what was observed for a daily time horizon (Section 4.1), no multi-feature clustering approach clearly outperforms the others in identifying process designs in the reduced scenario space. Nevertheless, considering higher central moments, e.g., up to kurtosis, for clustering leads on average to relatively similar results within the considered $N_{\text{scen, red}}$ range. Interestingly, multi-feature clustering based on principal components leads to process designs that are quite independent of $N_{\text{scen, red}}$ despite the significant variation of the objective function.

For the sake of completeness, the results of the sensitivity analysis for the remaining design variables are reported in Section 4.1 of Supporting Information.

4.2.2.2. Stand-alone Power-to-Methanol process.

Objective function

Fig. 11 displays the variation of the objective function evaluated on the reduced scenario space with respect to the number of scenario clusters for different clustering approaches.

In contrast to the grid-connected case study, the objective function shows a larger dependency on the number of scenario clusters. In particular, a higher $N_{\text{scen, red}}$ is necessary to obtain values that are less dependent on the number of clusters itself. This result aligns with previous works (Merrick, 2016): the convergence in the objective function needs more clusters when multiple stochastic variables are simultaneously considered (the PV and wind power generation in this case). Furthermore, such behavior can be partially explained by the guess on the size of the renewable power plants to perform DoF reduction, which introduces an error when the respective design variables also exhibit a dependency on $N_{\text{scen, red}}$ (see Section 3.2).

Further, the objective functions calculated through all clustering approaches do not always tend to the same value for the considered range of $N_{\text{scen, red}}$. This is particularly evident in Fig. 11 when comparing the results for k-medoids and k-means applied directly to the input time series. In fact, in contrast to k-medoids and multi-feature clustering, k-means clustering seems to generate excessively smooth representative scenario subsets, which are less suitable for estimating the objective function value with low $N_{\text{scen, red}}$. Among the multi-feature clustering approaches, the approach that considers the first four central moments leads to the objective function that is the least dependent on $N_{\text{scen, red}}$ when a sufficiently high number of clusters, e.g., eleven, are considered (Fig. 11). Similarly to the grid-connected case study, the clustering approach that considers the principal components performs the worst.

Design variables

Similarly to the grid-connected case study, the design variables exhibit a dependency on the number of scenario clusters. In particular, the size of the electrolysis, methanol synthesis, and storage units varies

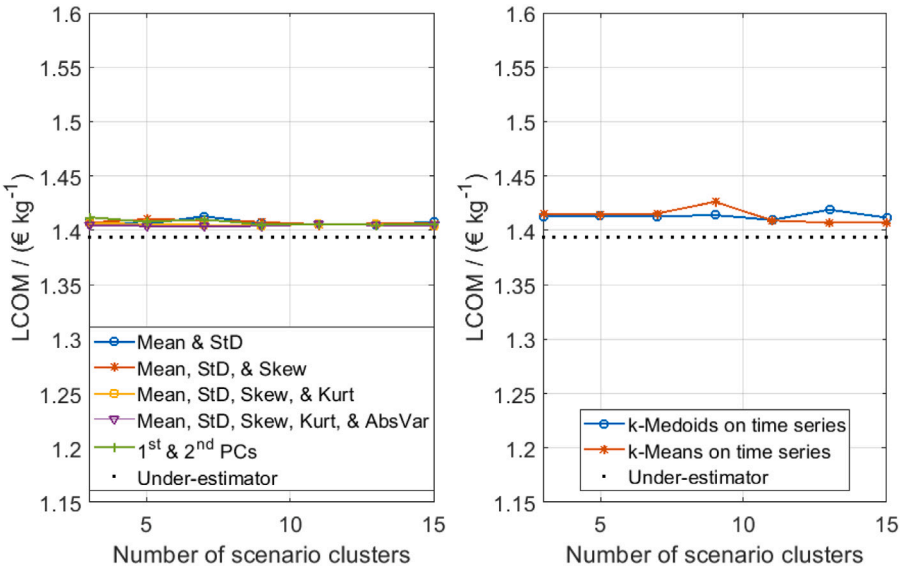


Fig. 8. Levelized cost of methanol for the grid-connected case study calculated by solving stochastic scheduling problems in the original scenario and DoF spaces for the process designs identified by solving reduced stochastic combined design and scheduling problems (LCOMs displayed in Fig. 7) for different numbers of weekly scenario clusters and different clustering approaches. Left: Multi-feature clustering via k-medoids based on mean, standard deviation (StD), skewness (Skew), kurtosis (Kurt), the mean of the absolute variation between consecutive time steps (AbsVar), and principal components (PCs). Right: k-medoids and k-means clustering applied to the original scenario time series. The black dotted line represents the under-estimator of the original two-stage stochastic problem. Note that the same *y*-axis scale as in Fig. 7 is used.

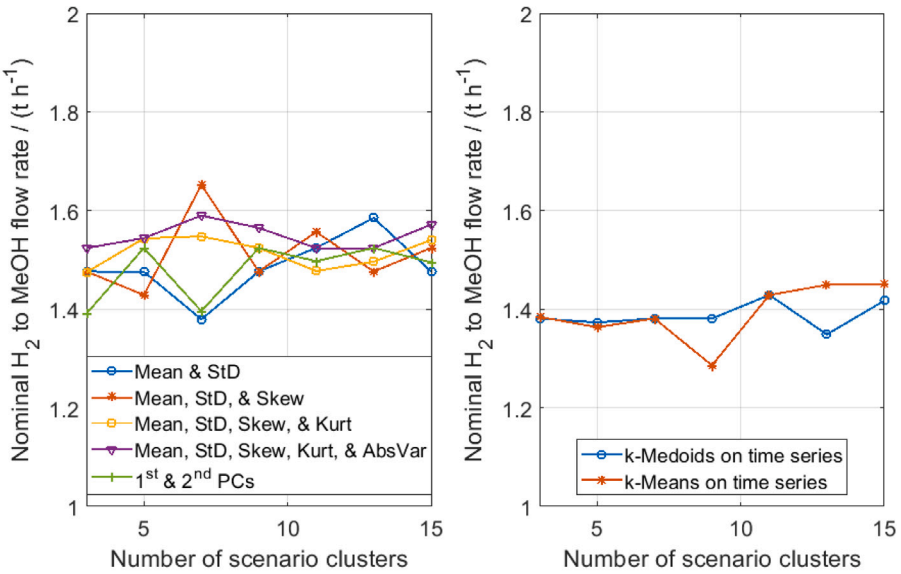


Fig. 9. Hydrogen flow rate to the methanol plant for the grid-connected case study for different numbers of weekly scenario clusters and clustering approaches. Left: Multi-feature clustering via k-medoids based on mean, standard deviation (StD), skewness (Skew), kurtosis (Kurt), the mean of the absolute variation between consecutive time steps (AbsVar), and principal components (PCs). Right: k-medoids and k-means clustering applied to the original scenario time series. Weekly scheduling horizons and degrees of freedom reduction ($N_{\mathrm{dof,\,sched}} = 18$) are applied.

significantly even for relatively high $N_{\mathrm{scen,\,red}}$. In contrast, some design variables, e.g., the nominal size of the PV and wind power plants, do not vary significantly when increasing $N_{\mathrm{scen,\,red}}$ (see for instance Fig. 12).

This variability in most design variables may be due to the input renewable power generation time series and how the reduced scenario set is obtained for relatively low $N_{\mathrm{scen,\,red}}$. In fact, when increasing $N_{\mathrm{scen,\,red}}$ starting from relatively low values, more extreme scenario profiles are selected. For such scenarios, large-size storage is generally more beneficial (Figs. 13 and 14), and this can affect not only the production cost but also the optimal process unit size.

For the sake of completeness, the results of the sensitivity analysis of the remaining design variables are reported in Section 4.2 of the Supporting Information.

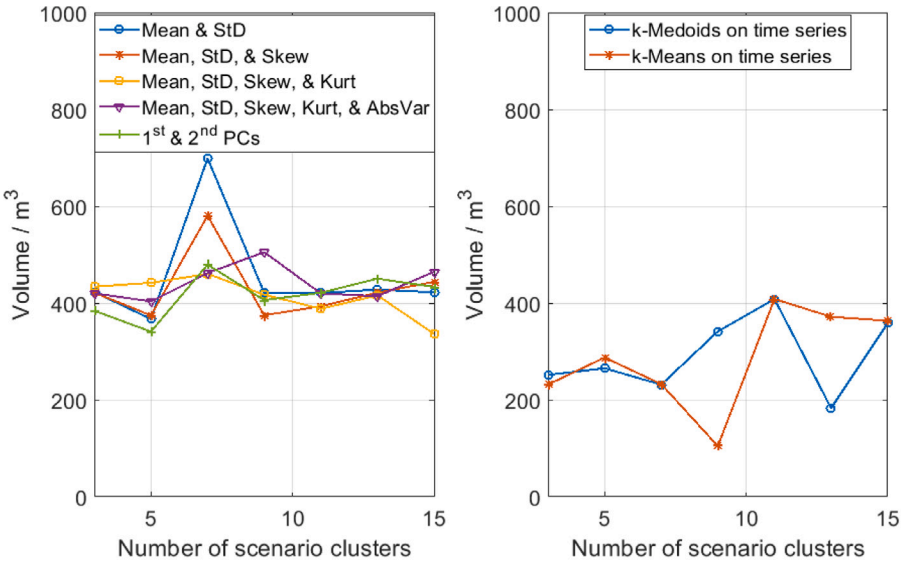


Fig. 10. Hydrogen storage volume for the grid-connected case study for different numbers of weekly scenario clusters and clustering approaches. Left: Multi-feature clustering via k-medoids based on mean, standard deviation (StD), skewness (Skew), kurtosis (Kurt), the mean of the absolute variation between consecutive time steps (AbsVar), and principal components (PCs). Right: k-medoids and k-means clustering applied to the original scenario time series. Weekly scheduling horizons and degrees of freedom reduction ($N_{\mathrm{dof,sched}} = 18$) are applied.

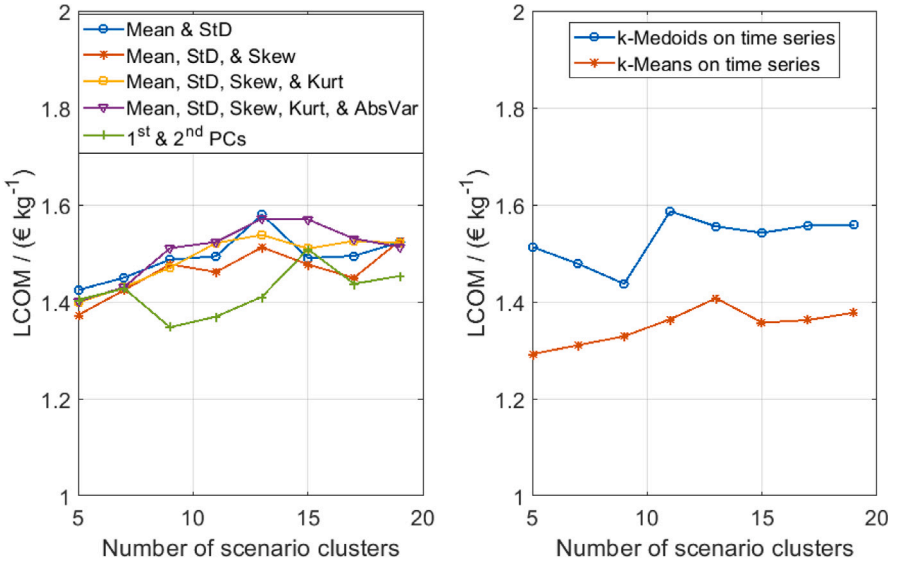


Fig. 11. Levelized cost of methanol for the stand-alone case study for different numbers of weekly scenario clusters and clustering approaches. Left: Multi-feature clustering via k-medoids based on mean, standard deviation (StD), skewness (Skew), kurtosis (Kurt), the mean of the absolute variation between consecutive time steps (AbsVar), and principal components (PCs). Right: k-medoids and k-means clustering applied to the original scenario time series. Weekly scheduling horizons and degrees of freedom reduction ($N_{\mathrm{dof,sched}} = 48$) are applied.

4.3. Discussion

Complexity reduction method applicability and performance

As shown in the previous sections, the investigated methodology, which combines feature-based scenario clustering with DoF reduction, has been applied to a Power-to-Methanol process with intermediate storage modeled as a MINLP. Nonetheless, this methodology can be applied to solve stochastic CDS optimization of other processes, e.g., other Power-to-X processes and energy systems, and for different process models, e.g., MILPs. In fact, the considered complexity reduction techniques are applied *ex-ante*: scenario clustering and the linear mapping for DoF reduction are performed without any prior knowledge about the process and model type, unless DoF reduction is applied selectively. For the latter case, considering information about the process is beneficial to select which scheduling variables should be linearly mapped.

Despite the general applicability of this methodology, its computational performance against other complexity reduction techniques might depend on the considered process and model type as well as

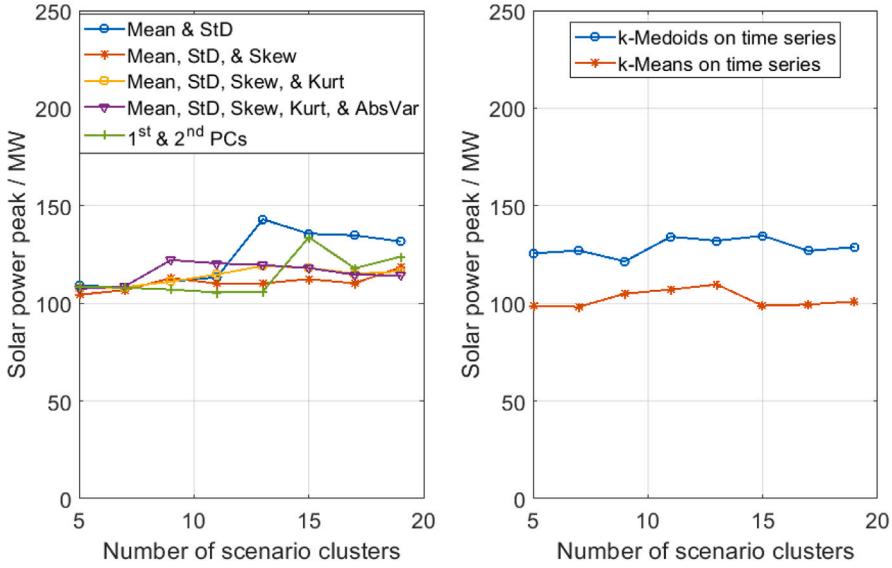


Fig. 12. Nominal capacity of the solar power plant for the stand-alone case study for different numbers of weekly scenario clusters and clustering approaches. Left: Multi-feature clustering via k-medoids based on mean, standard deviation (StD), skewness (Skew), kurtosis (Kurt), the mean of the absolute variation between consecutive time steps (AbsVar), and principal components (PCs). Right: k-medoids and k-means clustering applied to the original scenario time series. Weekly scheduling horizons and degrees of freedom reduction ($N_{\text{dof, sched}} = 48$) are applied.

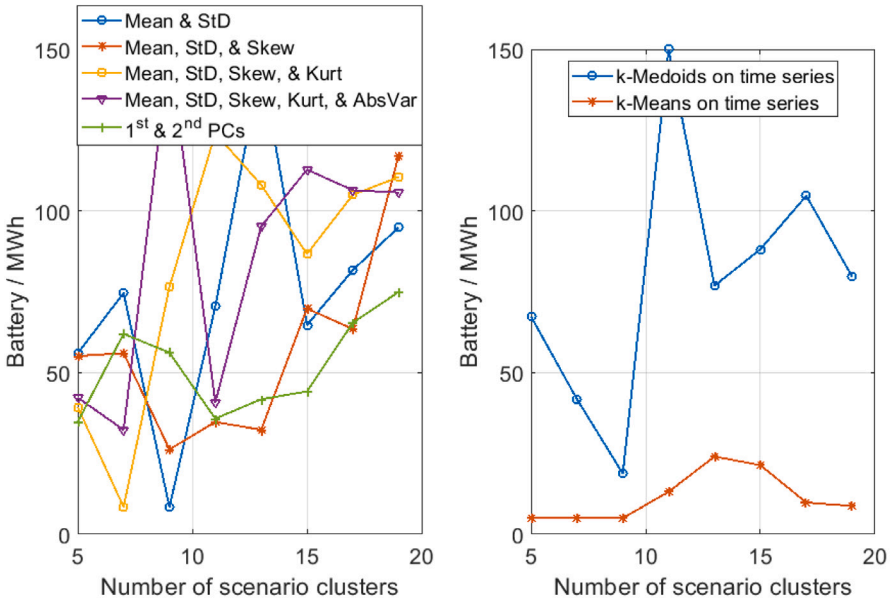


Fig. 13. Battery capacity for the stand-alone case study for different numbers of weekly scenario clusters and clustering approaches. Left: Multi-feature clustering via k-medoids based on mean, standard deviation (StD), skewness (Skew), kurtosis (Kurt), the mean of the absolute variation between consecutive time steps (AbsVar), and principal components (PCs). Right: k-medoids and k-means clustering applied to the original scenario time series. Weekly scheduling horizons and degrees of freedom reduction ($N_{\text{dof, sched}} = 48$) are applied.

solver, and it should therefore be evaluated on a case-by-case basis. In fact, even for the same process model, the computational benefits of using scenario clustering and DoF reduction are not always clear and consistent, although they reduce the overall number of optimization variables.

For the considered case studies, scenario clustering allows solving approximations of the original stochastic CDS optimization problem, for which BARON could not identify a feasible solution solvable within reasonable computational times. Moreover, the computational time needed by BARON to identify a feasible solution tends to increase when the number of scenario clusters increases and no DoF is applied (around 500 s, 2 000 s, and 40 000 s for the grid-connected PtMeOH case study with 3, 15, and 50 scenario clusters, respectively). However, it increases not monotonically when DoF reduction is applied (around 500 s, ca. 20 000 s, and 10 000 s for the grid-connected PtMeOH case study with 3, 15, and 50 scenario clusters, respectively). Further, the use of DoF reduction does not always lead to improved computational performance compared to considering the original time domain for the same number of scenario clusters. Finally, its performance seems to also depend on the considered solvers, which have different algorithms to identify feasible solutions and calculate model relaxations, and have been shown to react differently to reduced space formulations of optimization problems (Karia, 2024).

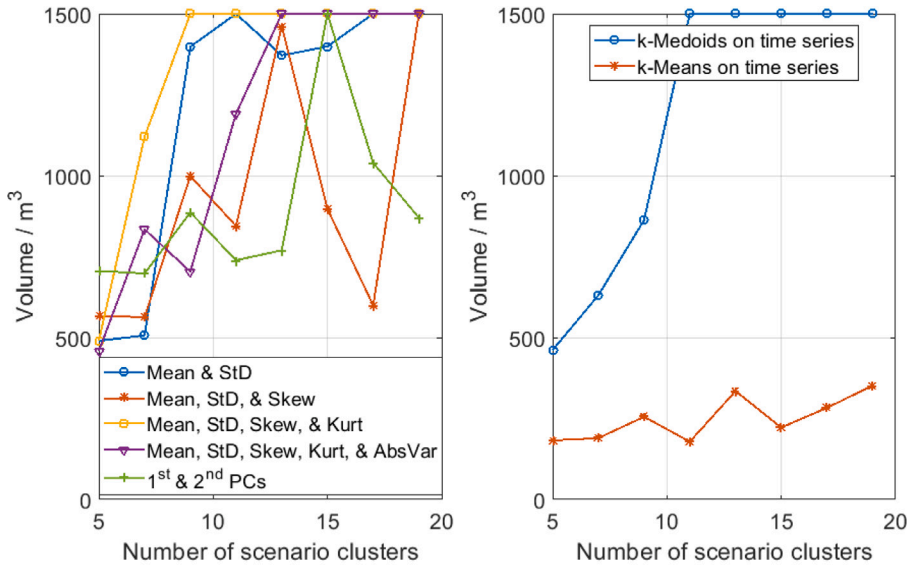


Fig. 14. Hydrogen storage volume for the stand-alone case study for different numbers of weekly scenario clusters and clustering approaches. Left: Multi-feature clustering via k-medoids based on mean, standard deviation (StD), skewness (Skew), kurtosis (Kurt), the mean of the absolute variation between consecutive time steps (AbsVar), and principal components (PCs). Right: k-medoids and k-means clustering applied to the original scenario time series. Weekly scheduling horizons and degrees of freedom reduction ($N_{\mathrm{dof,\,sched}} = 48$) are applied.

Clustering approaches: objective function vs. design variables

As shown for both grid-connected and stand-alone PtMeOH case studies, feature-based clustering can identify representative scenario subsets and probabilities to reduce the complexity of stochastic CDS problems: the objective function of the stochastic CDS problem in the reduced scenario and DoF domains becomes almost independent from the number of scenarios clusters already when considering a relatively low $N_{\mathrm{scen,\,red}}$ (see for instance the grid-connected case study in Section 4.2.2.1). In particular, considering the first four central moments provides on average the best results among the investigated multi-feature clustering approaches for both the grid-connected and stand-alone case studies. Furthermore, multi-feature clustering performs similarly or sometimes better than state-of-the-art clustering approaches, e.g., k-means applied to the time series. However, the best clustering approach is often problem-dependent (Kotzur et al., 2018; Phillips, 2024). Thus, multi-feature clustering should be tested for other case studies and time horizons in order to draw more robust conclusions.

In contrast to the objective function, the process design variables still exhibit a quite strong dependency on the number of scenario clusters even at high $N_{\mathrm{scen,\,red}}$. Nonetheless, these process designs, especially the designs identified via multi-feature clustering, perform well in the original scenario and DoF spaces as shown for the grid-connected PtMeOH case study (Fig. 8). One potential reason is that the objective function captures the trade-off between investment and operating costs and several process designs can lead to similar values (Conejo et al., 2010; Merrick, 2016; Baumgärtner et al., 2019a). This nexus between the process design and objective function is investigated in more detail in our recent work (Mucci and Bongartz, 2025).

Process design and operation implications

For both case studies and the considered economic assumptions (Appendix A.2) and irrespective of the clustering approach, all optimal process designs include oversizing the electrolysis and methanol synthesis units as well as the presence of hydrogen storage, thus confirming that PtMeOH processes should be designed to enable flexibility. The oversizing tends to be slightly higher for the stand-alone case study (ca. 20–30% vs. ca. 25–50% for the electrolysis unit of the grid-connected and stand-alone case study, respectively; ca. 15–30% vs. ca. 20–45% for the methanol synthesis unit of the grid-connected and stand-alone case study, respectively). Nonetheless, the exact extent is often different for the considered clustering approaches. Such differences can be due to the selection of representative scenario sets, the approximations related to DoF reduction, and the fact that different process designs can perform similarly well with respect to the objective function.

The optimal designs have bigger electrolysis and methanol synthesis units, as well as hydrogen storage (see Figs. 10 and 14), when multi-feature instead of k-medoids and k-means clustering approaches are considered. These process designs perform slightly better when solving stochastic scheduling problems in the original scenario and DoF spaces, as shown in Fig. 8 for the grid-connected PtMeOH process. These design choices were expected when scenarios are clustered via k-means, since it tends to smoothen the scenario profiles (Hoffmann et al., 2020; Kotzur et al., 2018) (also see Fig. A.1). In contrast, they were not necessarily expected for k-medoids clustering since it generally includes more profile variations (Kotzur et al., 2018).

In all results, the optimal maximum pressure ratio of the compression unit is close to the upper bound to store as much hydrogen as possible within the volume (see Section 4 of Supporting Information) so that electricity price and renewable power generation fluctuations can be better exploited to reduce the methanol production cost.

Under the considered economic assumptions (Appendix A.2), the optimization results suggest that battery storage is not economically beneficial for the grid-connected case study (value close to the lower bound in Figure S14 in Supporting Information), but beneficial for the stand-alone case study (Fig. 13). For the latter case, the large size of the battery might be explained by the upper bound reached for the hydrogen storage volume at high $N_{\mathrm{scen,\,red}}$, e.g., 15 (Fig. 14). In fact, hydrogen storage is generally preferred as storage medium over batteries as shown for the grid-connected case study (Section 4.2.2.1) and stand-alone case study with a daily time horizon (Subsection 3.2 of Supporting Information), since it allows increasing the capacity factor

of the downstream methanol synthesis plant. Nonetheless, the battery might play a major role at time scales shorter than the considered time discretization (1 h) and with the expected drop in their investment costs as already shown in our previous work (Mucci et al., 2023a). Further, the need for batteries might change in the case aging models for both the battery and electrolysis units are considered (not investigated in this work).

Finally, both power generation technologies are chosen by the optimizer in a solar-to-wind ratio of ca. 1:2 for the stand-alone case study. The combination of solar and wind power generation to minimize production costs aligns with literature works, e.g., Svitnič and Sundmacher (2022), and can be explained by the so-called complementarity of renewables: solar power generation tends to be higher than wind power generation in some periods of the year and vice versa, as shown, for example, for Germany (Densing and Wan, 2022). Nevertheless, a direct comparison between solar-to-wind ratios against other literature works cannot be performed, since it depends on the considered cost models and location.

Scenario horizon duration

When comparing the objective function variation within the considered $N_{\text{scen, red}}$ range and scenario horizon durations, the variability of the objective function value differs between the grid-connected and stand-alone case studies: for the grid-connected case study, the variability is slightly lower when long time horizons are considered (compare Figs. 5 and 7), while, for the stand-alone case study, it is higher when long time horizons are considered (compare Fig. 11 and Figure S6 in Supporting Information). For the grid-connected case study, this is most likely due to the frequency and duration of extreme events in the profiles: they are generally rare and of limited duration, thus playing a minor role over longer time horizons. For the stand-alone case study, this may be due to the additional fluctuations that renewable power generation has over longer time horizons combined with the increased utilization of storage technologies.

As mentioned above, the scenario horizon duration can affect storage size and its utilization. However, for the grid-connected case study, the optimal storage size calculated for a weekly and daily time horizon does not differ significantly (compare Fig. 10 and Figure S4 in Supporting Information). This result suggests that, for the considered PtMeOH process and input scenario space, hydrogen storage is used to deal with electricity price variations occurring within a few hours rather than to store large quantities of hydrogen. In contrast, for the stand-alone case study, the optimal size for storage calculated for a weekly and daily time horizon is significantly different (compare Fig. 14 and Figure S4 in Supporting Information). These results can be explained by the possibility of using storage to accommodate variations in intra-weekly renewable availability. Nonetheless, these assumptions should be confirmed by investigating longer time horizons.

5. Conclusions

We investigated feature-based scenario clustering for different sets of features (both interpretable and non-directly interpretable like central moments and principal components, respectively) to reduce the numerical complexity of multi-stage stochastic programming. We applied this approach to a stochastic combined design and scheduling optimization problem of a grid-connected and stand-alone Power-to-Methanol process with intermediate storage.

For a daily horizon, we found that the mean of the scenario profiles is the most relevant single feature for clustering to estimate the objective function. Nonetheless, single-feature scenario clustering is always outperformed by multi-feature scenario clustering for both case studies, in the sense that the latter can approximate the optimal objective value well with fewer clusters.

For a weekly horizon, we found that multi-feature clustering based on the first four central moments performs similarly or sometimes better than state-of-the-art clustering approaches, e.g., k-means, with respect to the objective function. In particular, the objective function exhibits a behavior that is almost independent of the scenario cluster number already with a small number of clusters (less than 10% of the original scenario space). A few more clusters are needed for the stand-alone case study than for the grid-connected case study to capture the correlation between the stochastic variables, i.e., solar and wind power generation.

As opposed to the objective function, the optimal design variables still exhibit a relatively strong dependency on the scenario cluster number, although the variations are lower when clustering based on several central moments, e.g., up to kurtosis. This might be due to the fact that several process designs can lead to similar levelized costs of methanol as shown for the grid-connected case study by solving stochastic scheduling problems for fixed process designs, since this objective function captures the trade-off between investment and operating costs. Further, the process designs obtained via feature-based clustering for relatively low scenario cluster numbers perform slightly better in the original scenario and DoF spaces than those obtained via k-medoids and k-means applied to the scenario time series.

Also, for the weekly horizon, we applied a degrees of freedom reduction approach tailored for scheduling variables that maintains the time step chronology memory to reduce the numerical complexity further. We found that DoF reduction should be applied selectively only to some scheduling variables, since the variable mapping introduces a strong correlation that can affect the optimal process design.

Although we showed the potential and effectiveness of feature-based clustering for single and multiple stochastic variables and different time horizons for TSO problems, the best clustering approach is generally problem-dependent (Kotzur et al., 2018; Phillips, 2024). Thus, feature-based clustering should be tested for longer time horizons, input scenario sets, problem formulations, e.g., risk-averse instead of risk-neutral optimization, and case studies. Nonetheless, using profile features that directly affect either the operating costs or the renewable power availability has the potential to perform well in other applications. Further, other features, e.g., belonging to the frequency domain and accounting for the peak and valley positions of the profiles, may also be worth investigating, since they can affect the scheduling.

Finally, while scenario clustering allows identifying representative stochastic problems that are solvable within reasonable times, the use of selective DoF reduction is not always numerically beneficial for the considered case studies, although it significantly reduces the number of optimization variables. This aspect could be affected by the numerical solver and the optimization problem numerics. Therefore, the computational improvements related to this approach should be evaluated on a case-by-case basis.

CRediT authorship contribution statement

Simone Mucci: Writing – original draft, Visualization, Software, Methodology, Investigation, Conceptualization. **Dominik Bongartz:** Writing – review & editing, Supervision, Methodology, Conceptualization.

Declaration of Generative AI and AI-assisted technologies in the writing process

During the preparation of this work, the authors used ChatGPT in order to improve the readability and language of the manuscript. After using this tool, the authors reviewed and edited the content as needed and take full responsibility for the content of the published article.

Declaration of competing interest

The authors declare that they have no known competing financial interests or personal relationships that could have appeared to influence the work reported in this paper.

Table A.1
Summary of the scenario clustering approaches for a single stochastic variable. Note that B is the matrix seen by the k-medoids method, C is the matrix with the cluster medoids and centroids, N_{TS}, N_{scen}, and $N_{scen,red}$ are the number of time steps per scenario, the number of scenarios, and the number of scenario clusters, respectively. Note that, for feature-based scenario clustering (approaches 1–11), the cluster medoids are used to identify the corresponding scenarios.

#	Approach	Matrix B	Matrix C
1	k-Medoids: Mean	$B \in \mathbb{R}^{1\times N_{scen}}$	$C \in \mathbb{R}^{1\times N_{scen,red}}$
2	k-Medoids: Standard deviation (StD)	$B \in \mathbb{R}^{1\times N_{scen}}$	$C \in \mathbb{R}^{1\times N_{scen,red}}$
3	k-Medoids: Skewness	$B \in \mathbb{R}^{1\times N_{scen}}$	$C \in \mathbb{R}^{1\times N_{scen,red}}$
4	k-Medoids: Kurtosis	$B \in \mathbb{R}^{1\times N_{scen}}$	$C \in \mathbb{R}^{1\times N_{scen,red}}$
5	k-Medoids: Mean absolute difference[a]	$B \in \mathbb{R}^{1\times N_{scen}}$	$C \in \mathbb{R}^{1\times N_{scen,red}}$
6	k-Medoids: 1st principal component	$B \in \mathbb{R}^{1\times N_{scen}}$	$C \in \mathbb{R}^{1\times N_{scen,red}}$
7	k-Medoids: Mean & StD	$B \in \mathbb{R}^{2\times N_{scen}}$	$C \in \mathbb{R}^{2\times N_{scen,red}}$
8	k-Medoids: Mean, StD, & Skewness	$B \in \mathbb{R}^{3\times N_{scen}}$	$C \in \mathbb{R}^{3\times N_{scen,red}}$
9	k-Medoids: Mean, StD, Skewness, & Kurtosis	$B \in \mathbb{R}^{4\times N_{scen}}$	$C \in \mathbb{R}^{4\times N_{scen,red}}$
10	k-Medoids: Mean, StD, Skewness, Kurtosis, & Mean absolute difference[a]	$B \in \mathbb{R}^{5\times N_{scen}}$	$C \in \mathbb{R}^{5\times N_{scen,red}}$
11	k-Medoids: 1st & 2nd principal components	$B \in \mathbb{R}^{2\times N_{scen}}$	$C \in \mathbb{R}^{2\times N_{scen,red}}$
12	k-Medoids: full time series	$B \in \mathbb{R}^{N_{TS}\times N_{scen}}$	$C \in \mathbb{R}^{N_{TS}\times N_{scen,red}}$
13	k-Means: full time series	$B \in \mathbb{R}^{N_{TS}\times N_{scen}}$	$C \in \mathbb{R}^{N_{TS}\times N_{scen,red}}$

[a] Mean absolute difference $= \sum_{t=2}^{N_{TS}} \frac{|x(t)-x(t-1)|}{N_{TS}-1}$.

Acknowledgments

The authors gratefully acknowledge the financial support by the German Federal Ministry of Research, Technology and Space (BMFTR) within the H2Giga project DERIEL (grant number 03HY122D). Further, the authors gratefully thank Erik Delarue, Marco Langiu, Chrysanthi Papadimitriou, Kristof Phillips, Jan F. Pyschik, J. Raphael Seidenberg, and Aron Zingler for fruitful discussions as well as Alexander Mitsos for valuable feedback on this work.

Appendix A

A.1. Considered scenario clustering approaches

In Table A.1, the considered scenario clustering approaches are listed. In particular, the scenario clustering approaches 1–6 apply k-medoids to single features, e.g., mean, extracted from the scenarios. The scenario clustering approaches 7–11 apply k-medoids to a matrix B where several features are combined. In contrast, the scenario clustering approaches 12 and 13 apply k-medoids and k-means directly to the original scenario time series.

Additional information on the size of the matrix B seen by the k-medoids and k-means clustering approaches as well as the corresponding cluster centers c is provided in Table A.1. Note that all cluster centers obtained via k-medoids belong to B, thus meaning that the scenarios corresponding to the centers belong to the original space, differently from cluster centers obtained via k-means.

As expected, considering different features for clustering leads to different scenario cluster centers and probabilities (see for instance Fig. A.1, where the cluster centers of four exemplary clustering approaches are shown).

A.2. Assumptions for the cost estimation of the Power-to-Methanol process with intermediate storage

The investment cost of the compression unit and the methanol synthesis plant is calculated according to the correlations in Biegler et al. (1997), which have a level of accuracy of 25–40%, by considering a corrective factor of 1.85 to account for fixed and working capital costs and a correction for inflation to the year 2023 via the chemical engineering plant cost index (CEPCI) (Maxwell, 2024). The investment costs of the other process units are estimated similarly to our previous work (Mucci et al., 2023a) by using technology-specific literature with the values updated to the year 2023. No salvage value is considered.

A summary of the considered specific investment costs can be found in Table A.2, while the main assumptions of the economic analysis are summarized in Table A.3.

A.3. Comparison of DoF reduction approaches

To determine a suitable number of DoFs, we solved the stochastic CDS problems for the grid-connected case study with three weekly scenarios obtained by clustering the electricity price profile for 2023 in Germany (ENTSO-E Transparency Platform, 2024) via k-medoids applied on the original time series. This clustering approach was chosen after preliminary optimization runs (see Section 4.1).

The results in Table A.4 show that reducing the DoF number $N_{dof,sched}$ from 168, i.e., the number of time steps N_{TS}, to 12 is already sufficient to approximate the objective function (error below 2% compared to the problem solved in the original time domain). However, the optimal design differs when DoF reduction is applied. In particular, the case where DoF reduction is applied to all scheduling variables leads to an optimal solution with no storage (design variables for storage at the lower bound).

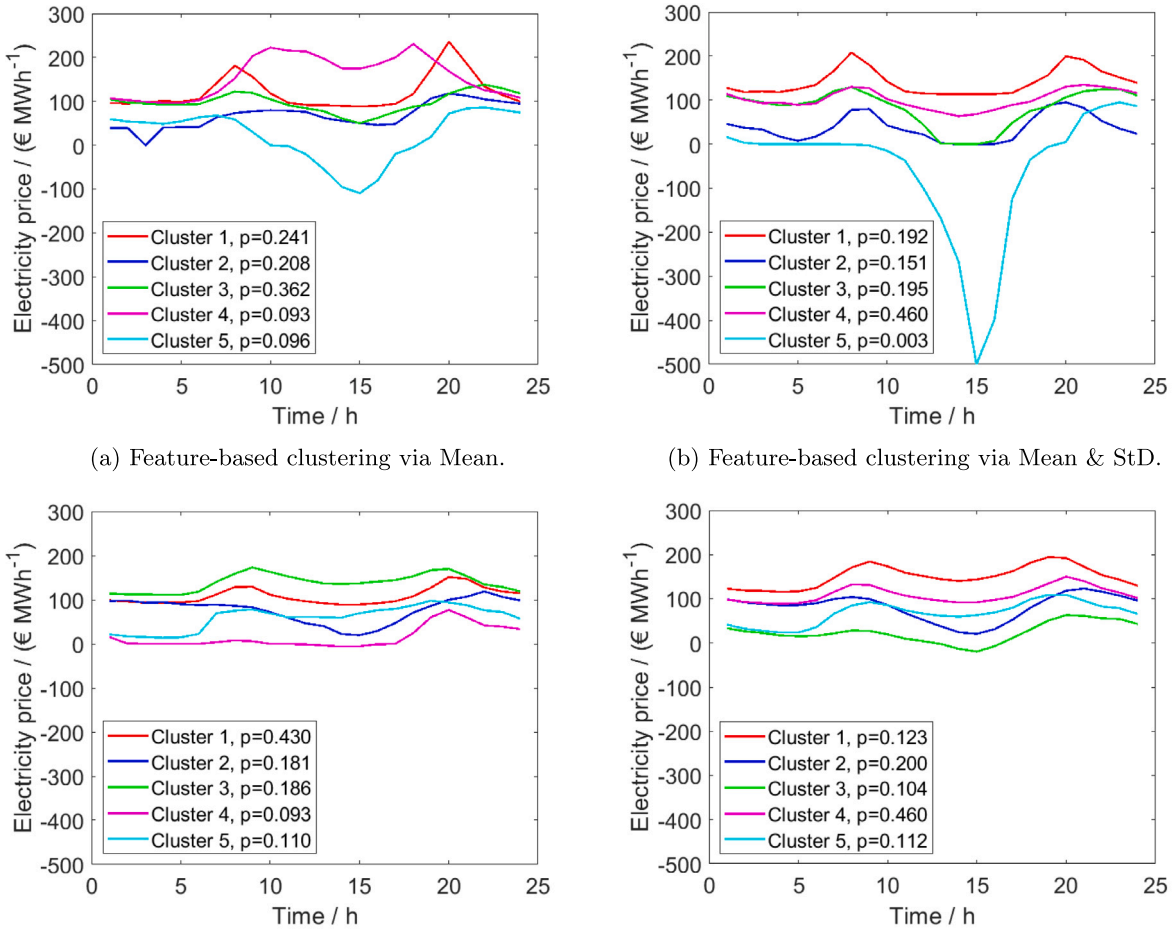
As already noticed for the stand-alone case study (see Section 4.2.1), the linear mapping introduces a strong correlation between scheduling variables, e.g., the power of the electrolyzer and the hydrogen supplied to the methanol synthesis plant ($\dot{m}_{H_2,MeOH}(t)$), thus leading to an optimal scheduling in which the produced hydrogen is converted directly into methanol instead of being partially stored in the hydrogen storage.

When the scheduling variable $\dot{m}_{H_2,MeOH}(t)$ is excluded from the linear mapping, the optimization problem has more optimization variables (3907 vs. 2971 for $N_{dof,sched} = 12$). Nevertheless, its solution shows the need for hydrogen storage and the objective function is improved (see Table A.4). The difference in the operation due to the hydrogen storage can be noticed in Fig. A.2, e.g., in the different PEM electrolyzer power demand, and by analogy the hydrogen production, and the hydrogen flow into the methanol synthesis plant.

The scheduling variables of the battery could also have been excluded from the linear mapping. However, this option has not been investigated here since the battery is often not chosen by the optimizer and its operation directly depends on the electricity prices used for defining the linear mapping matrix A_{dof}.

For $N_{dof,sched} = 18$, the error in the objective function value is below 1%, still achieving a reduction of the model variables higher than 50%. Thus, 18 DoFs were considered for generating the results of the grid-connected case study shown in Section 4.2.2.1.

When $\dot{m}_{H_2,MeOH}(t)$ is excluded from the linear mapping, the optimization problems solved for different ways of distributing the DoFs, i.e., excluding or not the time series extremes, have similar results concerning both the objective function and process design (see Table A.4). As there is no noticeable difference between the two approaches and the original weekly time series have several peaks and valleys that could potentially be clustered within the same DoF, we opted for clustering the input time series with $N_{dof,sched} = 18$ without handling the extremes differently.



(a) Feature-based clustering via Mean.

(b) Feature-based clustering via Mean & StD.

(c) k-medoids.

(d) k-means.

Fig. A.1. Daily electricity price profiles and their probability resulting from the clustering of day-ahead electricity prices for Germany in the year 2023 (ENTSO-E Transparency Platform, 2024). Figures (a) and (b) show the profiles obtained via feature-based clustering via mean and mean & standard deviation (StD), respectively. Figures (c) and (d) show the profiles obtained by clustering directly the original scenario time series via k-medoids and k-means applied to the original time series, respectively. (For interpretation of the references to color in this figure legend, the reader is referred to the web version of this article.)

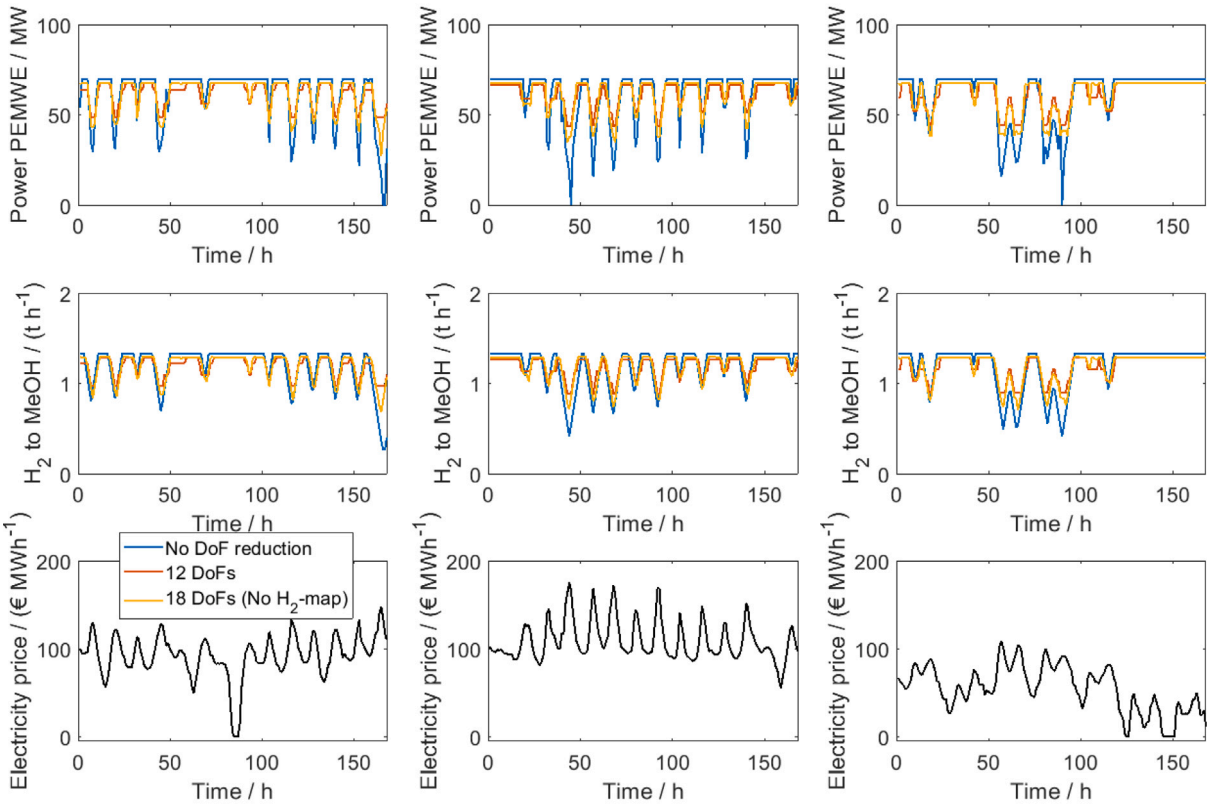
Table A.2
Considered values for the investment costs for the process units. The costs are referred to the year 2023.

	Values
PV power plant	0.70 M€/MW (IRENA, 2024)
Wind power plant	1.07 M€/MW (IRENA, 2024)
Utility-scale battery	0.31 M€/MWh (IEA, 2023)
PEM water electrolyzer[a]	1.21-1.27 M€/MW (Reksten et al., 2022)
Hydrogen vessel	8.8 k€/m^3 (U.S. Department of energy (DOE), 2024)
MeOH synthesis plant[b]	31.3 M€ (Mucci et al., 2023a)

[a] Size-dependent correlation; it includes a 1.75 factor for the auxiliaries.
[b] Reference plant with a yearly production of 0.08 Mt.

Table A.3
Main assumptions for the economic evaluation.

	Values
Operating weeks per year for the methanol synthesis plant	48 w/y
Lifetime of the Power-to-Methanol plant with storage	20 y
Yearly O&M as % of the initial $CAPEX_0$	5 %
Discount rate i	5 %
Reference year	2023
$ to € conversion factor	0.924
Cooling cost	0.1 €/MWh
CO_2 stream cost	50 €/t (IRENA and Methanol Institute, 2021)



(a) Scenario cluster 1. (b) Scenario cluster 2. (c) Scenario cluster 3.

Fig. A.2. Optimal solution of the two-stage stochastic problem for a grid-connected Power-to-Methanol plant when considering three weekly scenario clusters (Figures (a)–(c)) and different DoF reduction strategies (the three solid lines in the two upper graphs). In particular, the blue line represents the case where no DoF reduction is applied, the red line the case where DoF reduction is applied to all relevant scheduling variables and 12 DoFs are considered, and the yellow line the case where DoF reduction with 18 DoFs is applied to all relevant scheduling variables besides $\dot{m}_{H_{2,MeOH}}(t)$. (For interpretation of the references to color in this figure legend, the reader is referred to the web version of this article.)

Table A.4
Comparison of the objective function and the design variable values for different DoF reduction approaches applied to a two-stage stochastic problem of a grid-connected Power-to-Methanol process with intermediate storage. Three weekly electricity price scenario clusters of 168 h each are considered. The number of model variables as well as the NL_{code}, a GAMS indicator of the complexity for handling model nonlinearities, are also displayed. The results were extracted after 6 h CPU time. No global optimality was achieved.

$N_{dof,\,sched}$	Mapped scheduling variables	Specific cost of MeOH	En_{batt}	V	N_{mod}	β_{max}	$\dot{m}_{H_{2,MeOH,nom}}$	Model variables	NL_{code}
–		€/kg	MWh	m^3	–	–	t/h	–	–
168	None	1.46	5[a]	240	28	2.65	1.33	8587	31 822
12	All variables	1.46	5[a]	50[a]	27	1.88[a]	1.29	2971	11 698
12	All variables except for $\dot{m}_{H_{2,MeOH}}(t)$	1.46	5[a]	120	27	2.18	1.30	3907	11 698
12[b]	All variables except for $\dot{m}_{H_{2,MeOH}}(t)$	1.46	5	120	27	2.20	1.30	3907	11 698
18	All variables except for $\dot{m}_{H_{2,MeOH}}(t)$	1.46	5[a]	120	27	2.18	1.30	4087	12 472
18[b]	All variables except for $\dot{m}_{H_{2,MeOH}}(t)$	1.46	5[a]	120	27	2.19	1.29	4087	12 472

[a] At bound.
[b] The extremes have a dedicated DoF.

Appendix B. Supplementary data

Additional results, the Excel file, the Matlab script, and the GAMS model are available in the Supporting Material.

Supplementary material related to this article can be found online at https://doi.org/10.1016/j.cherd.2025.09.046.

References

Allman, A., Palys, M.J., Daoutidis, P., 2019. Scheduling-informed optimal design of systems with time-varying operation: A wind-powered ammonia case study. AIChE J. 65, http://dx.doi.org/10.1002/aic.16434.

Almaimouni, A., Ademola-Idowu, A., Kutz, J.N., Negash, A., Kirschen, D., 2018. Selecting and evaluating representative days for generation expansion planning. In: Power Systems Computation Conference. PSCC, IEEE, pp. 1–7. http://dx.doi.org/10.23919/PSCC.2018.8442580.

Bahl, B., Söhler, T., Hennen, M., Bardow, A., 2018. Typical periods for two-stage synthesis by time-series aggregation with bounded error in objective function. Front. Energy Res. 5, http://dx.doi.org/10.3389/fenrg.2017.00035.

Barandas, M., Folgado, D., Fernandes, L., Santos, S., Abreu, M., Bota, P., Liu, H., Schultz, T., Gamboa, H., 2020. TSFEL: Time series feature extraction library. SoftwareX 11, 100456. http://dx.doi.org/10.1016/j.softx.2020.100456.

Baumgärtner, N., Bahl, B., Hennen, M., Bardow, A., 2019a. RiSES[3]: Rigorous synthesis of energy supply and storage systems via time-series relaxation and aggregation.

Comput. Chem. Eng. 127, 127–139. http://dx.doi.org/10.1016/j.compchemeng.2019.02.006.
Baumgärtner, N., Temme, F., Hennen, M., Bahl, B., Hollermann, D., Bardow, A., 2019b. RiSES[4] rigorous synthesis of energy supply systems with seasonal storage by relaxation and time-series aggregation to typical periods. In: Simulation and Environmental Impact of Energy Systems. Wroclaw, Poland.
BDEW Bundesverband der Energie- und Wasserwirtschaft, 2025. Strompreisanalyse juli 2025 [online]. URL: https://www.bdew.de/service/daten-und-grafiken/bdew-strompreisanalyse/. [(last Access 06 October 2025)].
Belderbos, A., Delarue, E., 2015. Accounting for flexibility in power system planning with renewables. Int. J. Electr. Power Energy Syst. 71, 33–41. http://dx.doi.org/10.1016/j.ijepes.2015.02.033.
Biegler, L.T., Grossmann, I.E., Westerberg, A.W., 1997. Systematic Methods of Chemical Process Design. Prentice Hall PTR, pp. 110–174.
Bongartz, D., Mitsos, A., 2017. Deterministic global optimization of process flowsheets in a reduced space using McCormick relaxations. J. Global Optim. 69, 761–796. http://dx.doi.org/10.1007/s10898-017-0547-4.
Bruninx, K., Delarue, E., 2016. Scenario reduction techniques and solution stability for stochastic unit commitment problems. In: 2016 IEEE International Energy Conference. ENERGYCON, IEEE, pp. 1–7. http://dx.doi.org/10.1109/ENERGYCON.2016.7514074.
BSE engineering, 2025. Power-to-Methanol at small-scale: FlexMethanol 10&20 MW module [online]. URL: http://www.wfbe.de/BSE-Flyer-BASF-DB_web.pdf/. [(last Access 31 January 2025)].
Burre, J., Bongartz, D., Brée, L., Roh, K., Mitsos, A., 2020. Power-to-x: Between electricity storage, e-production, and demand side management. Chemie Ingenieur Tech. 92, 74–84. http://dx.doi.org/10.1002/cite.201900102.
Cao, Y., Laird, C.D., Zavala, V.M., 2016. Clustering-based preconditioning for stochastic programs. Comput. Optim. Appl. 64 (2), 379–406. http://dx.doi.org/10.1007/s10589-015-9813-x.
Caspari, A., Offermanns, C., Schäfer, P., Mhamdi, A., Mitsos, A., 2019. A flexible air separation process: 1. Design and steady-state optimizations. AIChE J. 65, http://dx.doi.org/10.1002/aic.16705.
Conejo, A.J., Carrión, M., Morales, J.M., 2010. Stochastic programming fundamentals. In: International Series in Operations Research and Management Science. Vol. 153, Springer New York LLC, pp. 27–62. http://dx.doi.org/10.1007/978-1-4419-7421-1_2.
De Sisternes, F.J., Webster, M.D., 2013. ESD working paper series: Optimal selection of sample weeks for approximating the net load in generation planning problems. URL: http://hdl.handle.net/1721.1/102959.
Densing, M., Wan, Y., 2022. Low-dimensional scenario generation method of solar and wind availability for representative days in energy modeling. Appl. Energy 306, 118075. http://dx.doi.org/10.1016/j.apenergy.2021.118075.
Dupačová, J., Gröwe-Kuska, N., Römisch, W., 2003. Scenario reduction in stochastic programming an approach using probability metrics. Math. Program. Ser. 95, 493–511. http://dx.doi.org/10.1007/s10107-002-0331-0.
Dvorkin, Y., Wang, Y., Pandzic, H., Kirschen, D., 2014. Comparison of scenario reduction techniques for the stochastic unit commitment. In: 2014 IEEE PES General Meeting | Conference & Exposition. IEEE, pp. 1–5. http://dx.doi.org/10.1109/PESGM.2014.6939042.
ENTSO-E Transparency Platform, 2024. Electricity prices and renewable power generation profiles [online]. URL: https://transparency.entsoe.eu/dashboard/show. [(last Access 30 September 2024)].
Gabrielli, P., Gazzani, M., Martelli, E., Mazzotti, M., 2018. Optimal design of multi-energy systems with seasonal storage. Appl. Energy 219, 408–424. http://dx.doi.org/10.1016/j.apenergy.2017.07.142.
Germscheid, S.H., Mitsos, A., Dahmen, M., 2024. Scenario reduction methods for risk-averse demand response scheduling under price uncertainty. Comput. Aided Chem. Eng. 53, 3223–3228. http://dx.doi.org/10.1016/B978-0-443-28824-1.50538-X.
Gorre, J., Ruoss, F., Karjunen, H., Schaffert, J., Tynjälä, T., 2020. Cost benefits of optimizing hydrogen storage and methanation capacities for Power-to-Gas plants in dynamic operation. Appl. Energy 257, 113967. http://dx.doi.org/10.1016/j.apenergy.2019.113967.
Heitsch, H., Römisch, W., 2003. Scenario reduction algorithms in stochastic programming. Comput. Optim. Appl. 24, 187–206. http://dx.doi.org/10.1023/A:1021805924152.
Heitsch, H., Römisch, W., 2009. Scenario tree reduction for multistage stochastic programs. Comput. Manag. Sci. 6, 117–133. http://dx.doi.org/10.1007/s10287-008-0087-y.
Helistö, N., Kiviluoma, J., Reittu, H., 2020. Selection of representative slices for generation expansion planning using regular decomposition. Energy 211, 118585. http://dx.doi.org/10.1016/j.energy.2020.118585.
Hoffmann, M., Kotzur, L., Stolten, D., Robinius, M., 2020. A review on time series aggregation methods for energy system models. Energies 13, 641. http://dx.doi.org/10.3390/en13030641.
Hu, J., Li, H., 2019. A new clustering approach for scenario reduction in multi-stochastic variable programming. IEEE Trans. Power Syst. 34, 3813–3825. http://dx.doi.org/10.1109/TPWRS.2019.2901545.
2023. World Energy Outlook 2023. Technical Report, Paris, URL: https://www.iea.org/reports/world-energy-outlook-2023.
2024. Renewable Generation Costs in 2023. Technical Report, Abu Dhabi, URL: https://www.irena.org/-/media/Files/IRENA/Agency/Publication/2024/Sep/IRENA_Renewable_power_generation_costs_in_2023.pdf.
2021. Innovation Outlook: Renewable Methanol. Technical Report, Abu Dhabi, URL: https://www.irena.org/publications/2021/Jan/Innovation-Outlook-Renewable-Methanol.
Jürgens, B., Seele, H., Schricker, H., Reinert, C., von der Assen, N., 2024. Decision-based vs. Distribution-driven clustering for stochastic energy system design optimization. ArXiv URL: http://arxiv.org/abs/2407.11457.
Karia, T., 2024. Tailored Formulations to Accelerate Deterministic Global Optimisation of Mixed-Integer Nonlinear Programs (Ph.D. thesis). Imperial College London, United Kingdom.
Karuppiah, R., Martín, M., Grossmann, I.E., 2010. A simple heuristic for reducing the number of scenarios in two-stage stochastic programming. Comput. Chem. Eng. 34, 1246–1255. http://dx.doi.org/10.1016/j.compchemeng.2009.10.009.
Khajavirad, A., Sahinidis, N.V., 2018. A hybrid LP/NLP paradigm for global optimization relaxations. Math. Program. Comput. 10, 383–421. http://dx.doi.org/10.1007/s12532-018-0138-5.
Kopp, M., Coleman, D., Stiller, C., Scheffer, K., Aichinger, J., Scheppat, B., 2017. Energiepark mainz: Technical and economic analysis of the worldwide largest power-to-gas plant with PEM electrolysis. Int. J. Hydrog. Energy 42, 13311–13320. http://dx.doi.org/10.1016/j.ijhydene.2016.12.145.
Kotzur, L., Markewitz, P., Robinius, M., Stolten, D., 2018. Impact of different time series aggregation methods on optimal energy system design. Renew. Energy 117, 474–487. http://dx.doi.org/10.1016/j.renene.2017.10.017.
Li, C., Grossmann, I.E., 2021. A review of stochastic programming methods for optimization of process systems under uncertainty. Front. Chem. Eng. 2, http://dx.doi.org/10.3389/fceng.2020.622241.
Liao, T.W., 2005. Clustering of time series data - A survey. Pattern Recognit. 38, 1857–1874. http://dx.doi.org/10.1016/j.patcog.2005.01.025.
Maggi, A., Bremer, J., Sundmacher, K., 2023. Multi-period optimization for the design and operation of a flexible Power-to-Methanol process. Chem. Eng. Sci. 281, 119202. http://dx.doi.org/10.1016/j.ces.2023.119202.
Martín, M., 2016. Methodology for solar and wind energy chemical storage facilities design under uncertainty: Methanol production from CO_2 and hydrogen. Comput. Chem. Eng. 92, 43–54. http://dx.doi.org/10.1016/j.compchemeng.2016.05.001.
Maxwell, C., 2024. Cost indices [online]. URL: https://toweringskills.com/financial-analysis/cost-indices/. [(last Access 25 September 2024)].
Merrick, J.H., 2016. On representation of temporal variability in electricity capacity planning models. Energy Econ. 59, 261–274. http://dx.doi.org/10.1016/j.eneco.2016.08.001.
Mitsos, A., Asprion, N., Floudas, C.A., Bortz, M., Baldea, M., Bonvin, D., Caspari, A., Schäfer, P., 2018. Challenges in process optimization for new feedstocks and energy sources. Comput. Chem. Eng. 113, 209–221. http://dx.doi.org/10.1016/j.compchemeng.2018.03.013.
Mößle, P., Herrmannsdörfer, T., Welzl, M., Brüggemann, D., Danzer, M.A., 2025. Economic optimization for the dynamic operation of a grid-connected and battery-supported electrolyzer. Int. J. Hydrog. Energy 100, 749–759. http://dx.doi.org/10.1016/j.ijhydene.2024.12.216.
Mucci, S., Bongartz, D., 2025. Stochastic optimization of Power-to-Methanol: Production cost sensitivity to process design vs. scheduling. Submitted.
Mucci, S., Mitsos, A., Bongartz, D., 2023a. Cost-optimal Power-to-Methanol: Flexible operation or intermediate storage? J. Energy Storage 72, 108614. http://dx.doi.org/10.1016/j.est.2023.108614.
Mucci, S., Mitsos, A., Bongartz, D., 2023b. Power-to-x processes based on PEM water electrolyzers: A review of process integration and flexible operation. Comput. Chem. Eng. 175, 108260. http://dx.doi.org/10.1016/j.compchemeng.2023.108260.
Papadimitriou, C., Schulze, J.C., Mitsos, A., 2025. A practical scenario generation method for electricity prices on day-ahead and intraday spot markets. Comput. Chem. Eng. 199, 109118. http://dx.doi.org/10.1016/j.compchemeng.2025.109118.
Papadimitriou, C., Varelmann, T., Schröder, C., Jupke, A., Mitsos, A., 2023. Globally optimal scheduling of an electrochemical process via data-driven dynamic modeling and wavelet-based adaptive grid refinement. Optim. Eng. http://dx.doi.org/10.1007/s11081-023-09860-6.
Pfenninger, S., 2017. Dealing with multiple decades of hourly wind and PV time series in energy models: A comparison of methods to reduce time resolution and the planning implications of inter-annual variability. Appl. Energy 197, 1–13. http://dx.doi.org/10.1016/j.apenergy.2017.03.051.
Phillips, K., 2024. Efficiently Capturing Spatio-Temporal Variability in Power System Planning Models (Ph.D. thesis). KU Leuven, Belgium.
Poncelet, K., Hoschle, H., Delarue, E., Virag, A., D'haeseleer, W., 2017. Selecting representative days for capturing the implications of integrating intermittent renewables in generation expansion planning problems. IEEE Trans. Power Syst. 32, 1936–1948. http://dx.doi.org/10.1109/TPWRS.2016.2596803.
Raheli, E., Werner, Y., Kazempour, J., 2023. A conic model for electrolyzer scheduling. Comput. Chem. Eng. 179, 108450. http://dx.doi.org/10.1016/j.compchemeng.2023.108450.
Raya-Tapia, A.Y., López-Flores, F.J., Tovar-Facio, J., Ponce-Ortega, J.M., 2025. Comparative framework of representative weeks selection methods for the optimization of power systems. Comput. Chem. Eng. 194, 108985. http://dx.doi.org/10.1016/j.compchemeng.2024.108985.

Reksten, A.H., Thomassen, M.S., Møller-Holst, S., Sundseth, K., 2022. Projecting the future cost of PEM and alkaline water electrolysers; a CAPEX model including electrolyser plant size and technology development. Int. J. Hydrog. Energy 47 (90), 38106–38113. http://dx.doi.org/10.1016/j.ijhydene.2022.08.306.

Schäfer, P., Schweidtmann, A.M., Lenz, P.H., Markgraf, H.M., Mitsos, A., 2020a. Wavelet-based grid-adaptation for nonlinear scheduling subject to time-variable electricity prices. Comput. Chem. Eng. 132, http://dx.doi.org/10.1016/j.compchemeng.2019.106598.

Schäfer, P., Schweidtmann, A.M., Mitsos, A., 2020b. Nonlinear scheduling with time-variable electricity prices using sensitivity-based truncations of wavelet transforms. AIChE J. 66, http://dx.doi.org/10.1002/aic.16986.

Schiffer, Z.J., Manthiram, K., 2017. Electrification and decarbonization of the chemical industry. Joule 1, 10–14. http://dx.doi.org/10.1016/j.joule.2017.07.008.

Sun, M., Teng, F., Zhang, X., Strbac, G., Pudjianto, D., 2019. Data-driven representative day selection for investment decisions: A cost-oriented approach. IEEE Trans. Power Syst. 34 (4), 2925–2936. http://dx.doi.org/10.1109/TPWRS.2019.2892619.

Svitnič, T., Sundmacher, K., 2022. Renewable methanol production: Optimization-based design, scheduling and waste-heat utilization with the FluxMax approach. Appl. Energy 326, 120017. http://dx.doi.org/10.1016/j.apenergy.2022.120017.

Teichgraeber, H., Brandt, A.R., 2019. Clustering methods to find representative periods for the optimization of energy systems: An initial framework and comparison. Appl. Energy 239, 1283–1293. http://dx.doi.org/10.1016/j.apenergy.2019.02.012.

Teichgraeber, H., Brandt, A.R., 2020. Optimal design of an electricity-intensive industrial facility subject to electricity price uncertainty: Stochastic optimization and scenario reduction. Chem. Eng. Res. Des. 163, 204–216. http://dx.doi.org/10.1016/j.cherd.2020.08.022.

Teichgraeber, H., Lindenmeyer, C.P., Baumgärtner, N., Kotzur, L., Stolten, D., Robinius, M., Bardow, A., Brandt, A.R., 2020. Extreme events in time series aggregation: A case study for optimal residential energy supply systems. Appl. Energy 275 (January), 115223. http://dx.doi.org/10.1016/j.apenergy.2020.115223.

U.S. Department of energy (DOE), 2024. Technical targets for hydrogen delivery [online]. URL: https://www.energy.gov/eere/fuelcells/doe-technical-targets-hydrogen-delivery. [(last Access 04 October 2024)].

Wajeh, M.E., Mhamdi, A., Mitsos, A., 2024. Optimal design and flexible operation of a fully electrified biodiesel production process. Ind. Eng. Chem. Res. 63, 1487–1500. http://dx.doi.org/10.1021/acs.iecr.3c03074.

Zhang, Y., Cheng, V., Mallapragada, D.S., Song, J., He, G., 2023. A model-adaptive clustering-based time aggregation method for low-carbon energy system optimization. IEEE Trans. Sustain. Energy 14 (1), 55–64. http://dx.doi.org/10.1109/TSTE.2022.3199571.

Zhang, Q., Grossmann, I.E., 2016. Enterprise-wide optimization for industrial demand side management: Fundamentals, advances, and perspectives. Chem. Eng. Res. Des. 116, 114–131. http://dx.doi.org/10.1016/j.cherd.2016.10.006.